HOKKAIDO UNIVERSITY

Title	ANALYSIS AND CONTROL FOR RANDOM ERROR OF NIGHT TIME POSITION LINE IN HOKKAIDO DECCA CHAIN
Author(s)	KAWAGUCHI, SHINICHIRO
Citation	MEMOIRS OF THE FACULTY OF FISHERIES HOKKAIDO UNIVERSITY, 26(1-2), 1-48
Issue Date	1979-03
Doc URL	https://hdl.handle.net/2115/21866
Type	departmental bulletin paper
File Information	26(1_2)_P1-48.pdf

Hokkaido University Collection of Scholarly and Academic Papers : HUSCAP

ANALYSIS AND CONTROL FOR RANDOM ERROR OF NIGHT TIME POSITION LINE IN HOKKAIDO DECCA CHAIN

SHINICHIRO KAWAGUCHI

Faculty of Fisheries, Hokkaido University, Hakodate, Japan

Content

Page

1. Introduction 2
2. Time series analysis of random error series of night time position line 5
   - 2–1 Method of measurement 5
   - 2–2 The range of variation for random error series of night time position line .. 6
   - 2–3 The results of time series analysis for random error series of the Decca system 7
   - 2–4 Comparison of statistical characteristics of random error series of night time position line between two observational points in the frequency domain .. 10
   - 2–5 The time-constant and the band-width of random error series of position line 17
   - 2–6 The relationship between maxima and slip-lane for random error series of night time position line 19
3. Time series analysis between field strength and position line. 20
   - 3–1 Probability density function of the envelope and the phase for composite wave of ground wave plus sky wave 20
   - 3–2 Frequency response characteristics between time series of position line and the one of field strength from master and slave stations 22
   - 3–3 The results of time series analysis between field strength, which is transmitting from master and slave stations, and position line 24
4. Real time adaptive control for random error series of position line which is observed at a fixed point at night 28
   - 4–1 Formulation of adaptive control process for random error series which is observed at a fixed point 28
   - 4–2 Auto regressive model for random error series of night time position line 29
   - 4–3 Auto regressive prediction for random error series of night time position line 30
   - 4–4 The scheme of adaptive control for random error series of night time position line at a fixed point by monitoring method 31
   - 4–5 The relationship between the estimation function and error ellipse 32
   - 4–6 The ideal frequency response function on the occasion of the estimation for the results of real time adaptive control in the frequency domain 34
   - 4–7 The results of adaptive control for random error series of night time position line at a fixed point by monitoring method 35
   - 4–8 Time-space coverage of auto regressive model at monitoring points 44
5. Conclusion 46

Reference 47

1. Introduction

The Decca navigational system was developed in England during World War II and it is used outside Japan as a navigational aid. It is a continuous-wave phase comparison system operating in the frequency range from 70 to 130 KHz. It is a hyperbolic system and three synchronized station are necessary for a fix. 290 vessels which consist chiefly in trawl-boats install the Decca receiver in the Hokkaido Decca chain, and 95% of them are fishing ones. A part of the Decca receiver in the fishing boat is not so much a navigational aid as the fishing gear in a wide sense, so it is used to determine the relative position to the fishing shoals.

The Decca system which determines the lane by measuring the phase difference of the electro-magnetic wave between master and slave stations is able to obtain sufficient accuracy as fishing gear in the day time (Fig. 1–1). But at night we can't obtain sufficient accuracy on account of skywave interference, and a broad area in which we can't use the Decca system comes out. This means a great loss to the efficiency of the Decca system which keeps high accuracy of a ship's position (Fig. 1–2). The reason why the night time variation of position line for Decca system interferes with the decision of a ship's position is due to the impossibility of night time skywave correction as the Loran and Omega system.

Researches of the variation of position line at the Hokkaido Decca chain have been made by The Maritime Safety Agency.[1)2)3)4)5)] For the purpose of getting fundamental data which help construct the Hokkaido Decca chain. The Maritime Safety Agency has been reserched characteristics of the propagation from 70 to 130KHz since 1960, and constant error of position line has been improved tolerably (Fig. 1–3). On account of these investigations, the Decca correction chart has been published in 1968.[6)] But scarcely any prevention measures have been taken against random error series of night time position line.

An elimination of night time variation of position line at the transmitting station is obtained as follows;

(1) Development of antenna which can eliminate the component of sky wave completely.

(2) Arrangement of the phase which is adaptive for real time variation of apparent height of the ionospheric gradient.

But they can't work out countermeasures with technical difficulties.

On the other hand, the study of the problem at our user's side might be best to work out prediction and control using the results of statistical characteristics of a position line in the frequency domain.

Chapter 2 of this study first describes general statistics of night time variation of position line for the Decca system (2–2 to 2–4). In section 2–6, a power spectrum of random error series of night time position line which is an important characteristics in the frequency domain is described, and frequency response characteristics between two observational points. Section 2–7 describes Time-constant and band-width which are related to the index of the estimation of the result for adaptive control. The chapter ends with a description of how the amplitude of maxima may be used in slip-lane in the Decca system.

Section 3–1 discusses the joint probability density function and independence between the envelope and the phase. In section 3–2, the main object is the consideration of two input linear system frequency response function and associated applications of cohereny function, where the inputs are time series of field strength from master and slave stations and the output is one of the position line. Section

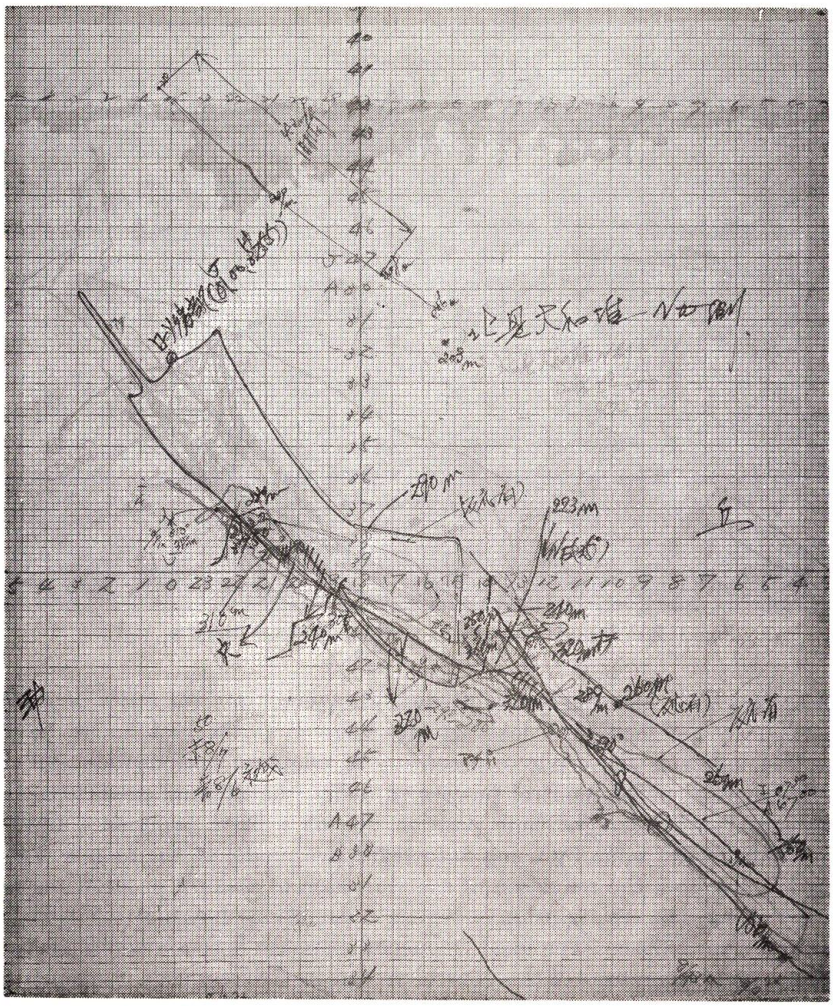

Fig. 1–1. Typical example of plotting of Decca track on trowling.

3–3 describes the results of the time series analysis between field strength and position line.

Section 4–1 describes formation of a statistical adaptive control process for random error series of night time position line. In section 4–2, we consider a

simplified discrite time model in which data are available only at equal intervals of time each of which we call a phase. The identification of this model is realized by fitting auto regressive model of successive orders within a prescribed range, computing estimates of FPE (final prediction error) for the model, and adopting the one with the minimum of the estimates.

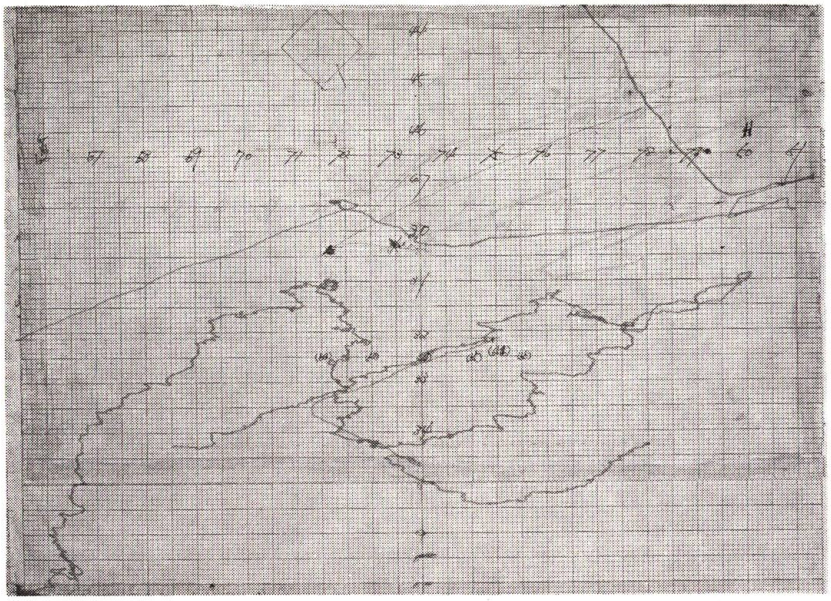

Fig. 1–2. Typical example of plotting of Decca track at night.

In section 4–3, auto regressive prediction of random error series of night time position line by the method of least squares is given as the best linear prediction. Section 4–4 indicates the concrete procedure of adaptive optimization and control. It is the purpose of this control process to define the optimal prediction value of random error series of night time position line at a fixed point as a function of previous data of the same by using auto regressive model at the monitoring point. Section 4–5 describes the reduction of the viariation of a ship's position mathematically by using the relationship between estimation function of this control process and error ellipse. The ideal frequency response function which is used for the estimation of the results of this control process in the frequency domain is defined in section 4–6. Section 4–7 explains in details the result of the adaptive control for random error series of night time position line which is measured at a fixed point in the sea. The chapter ends with the description of time-space coverage of auto regressive model at the monitoring points.

Before going further, the author wishes to express his hearty thanks to Professor M. Ishida, Professor R. Kawashima and Associate Professor T. Suzuki,

Lecture N. Sano of the faculty of Fisheries Hokkaido University, for their helpful guidance and criticism in regard to the probrem discussed in this paper.

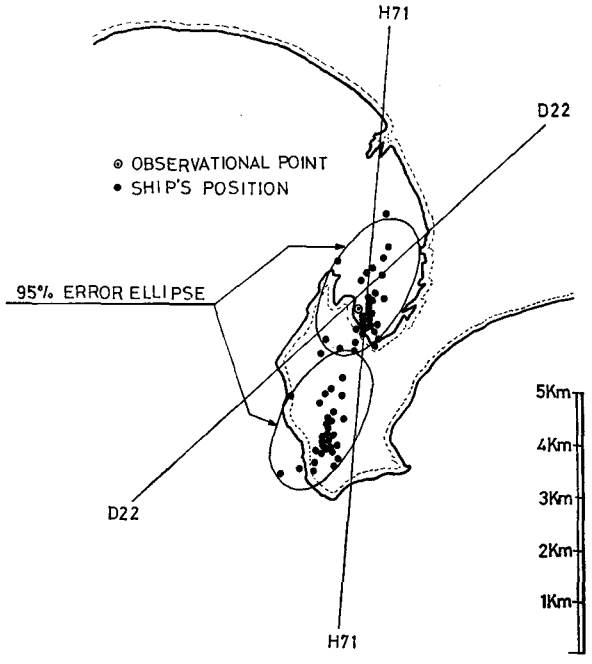

Fig. 1–3. Relationship between constant error and random error.

2. Time series analysis of random error series of night time position line[7)8)]

2-1 Method of measurement

The measurement which lies in the use of a 8 mm camera and an interval timer is done every minute from 4:30 P.M. to 7:30 A.M. The main observational points which were chosen so as to cover the whole Hokkaido at a minimum are Hakodate, Kushiro and Wakkanai (Fig. 2–1). A term of measurement is done as follows;

(1) February 2–4, 1976
(2) May 10–13, 1976
(3) June 14–16, 1976
(4) October 13–15, 1976

also other observational points were chosen irregularly as follows;

(5) October 15–16, 1975 at Monbetsu
(6) July 14–16, 1976 at Rishiri
(7) July 18–20, 1976 at Shakotan

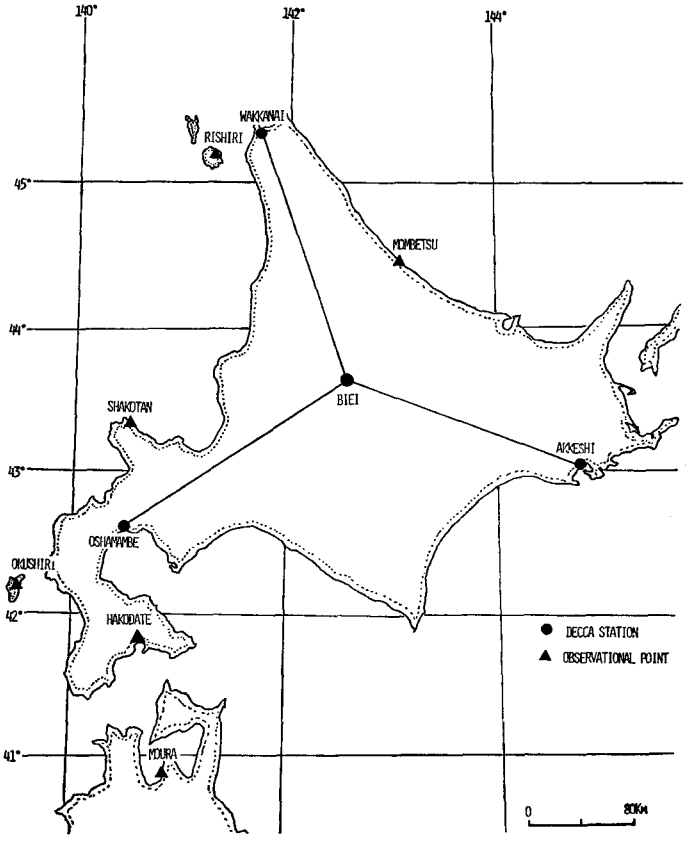

Fig. 2–1. Configuration of Hokkaido Decca chain and observational points.

(8) July 27–29, 1976 at Okushiri
(9) August 11–13, 1976 at Moura

2-2 The range of variation for random error series of night time position line

Fig. 2–2 to Fig. 2–4 show the random error series of night time position line at Hakodate, Kushiro and Wakkanai by actual measurement, and zero is equal to the arithmetic mean. It has been definitely shown by these Figures that it shows the characteristics of continious LF band, at which ground wave is prior to sky wave within the coverage of Lane Identification. Table 2–1 indicates the standard deviation and confidence limits of random error at three observational points. It has been evident by this table that the standard deviation of random error series of night time position line shows the seasonal variation which has this tendency: summer>autumn, spring>winter. It has been reported that the phase variation of LF band depends on the ionospheric gradient, so the variation of apparent

height of the ionosphere is very important as parameter on the occasion of building a structural model for random error series of night time position line.

The measurement of ionosphere is done by The Radio Research Laboratories and the critical frequency and apparent height of Es, F1 and F2 have been reported every month.[9] But the band-width of this measurement is from 1 MHz

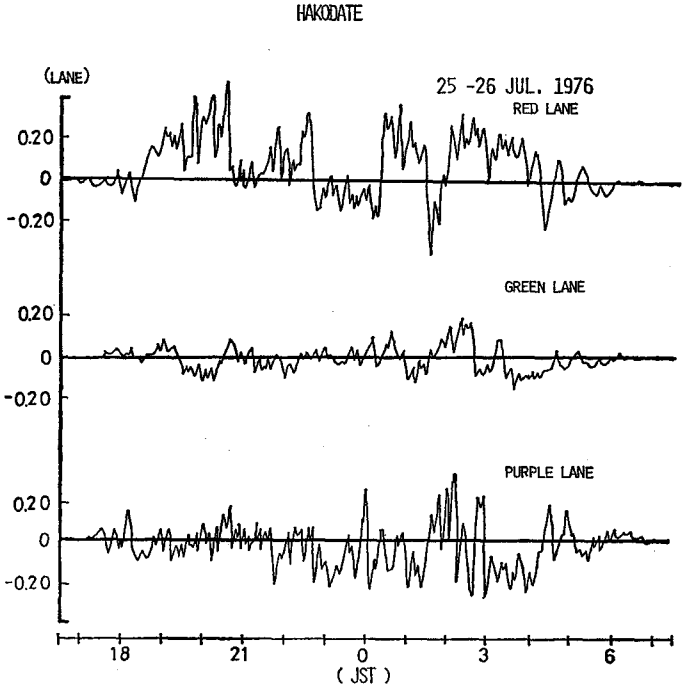

Fig. 2–2. Random error series of night time position line at Hakodate.

to 25 MHz, so we can't obtain the propagation characteristics of the LF band. This is why we investigate the frequency response characteristics between field strength and position line. We make a detailed explanation of the response characteristics between field strength and position line in Chapter 3.

2-3 The results of time series analysis for random error series of the Decca system

The random error of position line has been constantly considered as the range of variation. But we have the relation

$$\delta_x = \sqrt{\int_{-\infty}^{\infty} P(\omega)\, d\omega} \qquad (2\text{–}1)$$

where δ_x: standard deviation of random error
$p(\omega)$: power spectrum of random error

So it is natural to consider in detail the power component of variation of position line in the frequency domain.

Given a set of data which is stationary and Gaussian stochastic process $Z(s)$; $s=1, 2, 3, \cdots N$, autocorrelation function Czz (τ) of random error series of night time position line is given by

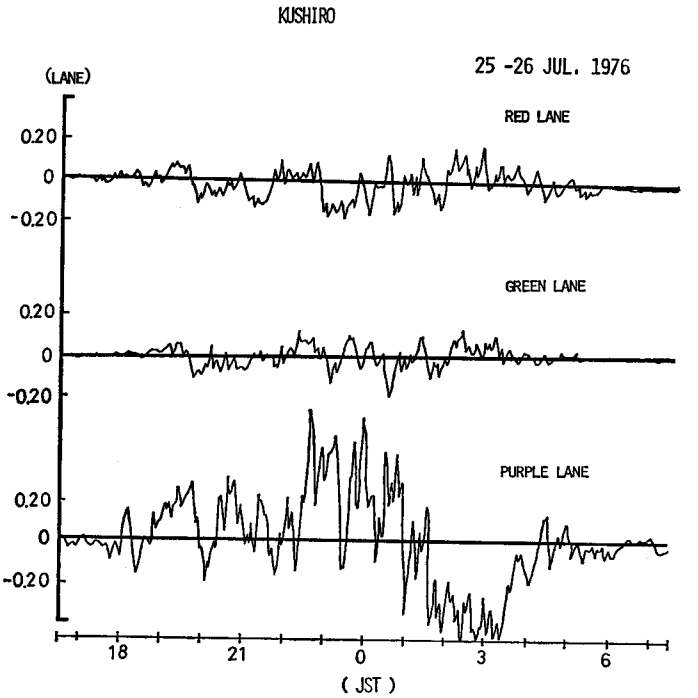

Fig. 2-3. Random error series of night time position line at Kushiro.

$Z(s)$; $s=1, 2, 3, \cdots, N$

$$C_{zz}(\tau) = \frac{1}{N} \lim_{N\to\infty} \sum_{\tau=1}^{N-l} \{Z(s+\tau)-m_z\}\{Z(s)-m_z\} \qquad (2\text{-}2)$$

where $$m_z = \lim_{N\to\infty} \frac{1}{N} \sum_{s=1}^{N} Z(s)$$

and power spectrum $P(\omega)$ is defined as the Fourier Transform $C_{zz}(\tau)$

$$\overline{P(\omega)} = \frac{1}{2\pi} \int_{-\infty}^{\infty} C_{zz}(\tau) \exp(-j\omega\tau)\, d\tau \qquad (2\text{-}3)$$

Furthermore we smooth $\overline{P(\omega)}$ by smoothing the coefficient to obtain

$$P(\omega) = 0.25\overline{P(\omega_{k-1})} + 0.5\overline{P(\omega_k)} + 0.25\overline{P(\omega_{k+1})} \qquad (2\text{–}4)$$

Fig. 2–5 give the results of application of this procedure for random error series of night time position line for the Decca system. It is found that the random error series consist of much low-frequency components and few high-frequency components.

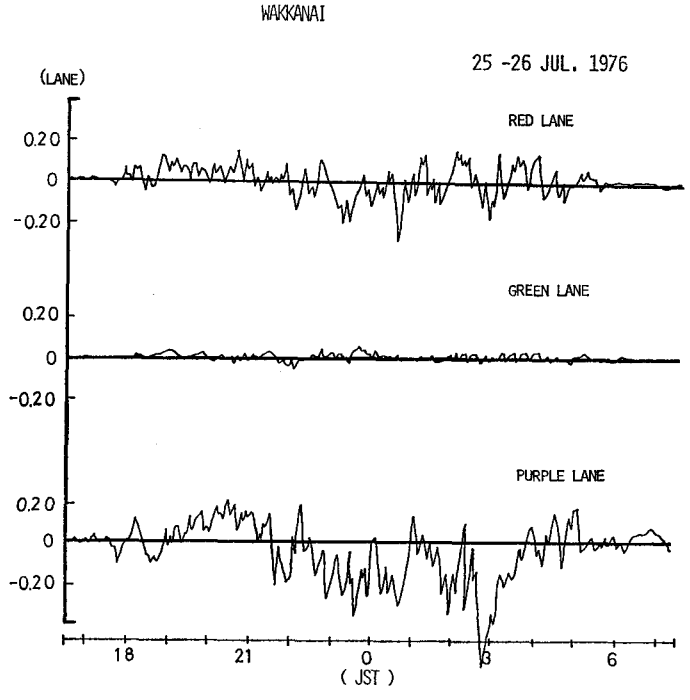

Fig. 2–4. Random error series of night time position line at Wakkanai.

The power component of Green lane is the smallest of the three through the whole frequency range and 30% of them have no power in high frequency range. These facts indicate the stability of the position line of Green lane. The proper explanation of stability of the position line of Green lane has not been reported by The Maritime Safety Agency. The major causes for the facts are given as follows;

(1) The location of the transmitting station at Wakkanai is in the best condition compared with other stations.

(2) Propagation characteristics of $9f_0$ is the most stable of the three ($9f_0$, $8f_0$, $5f_0$).

(3) The multiple number of $9f_0$ is the smallest of the three.

The smallest power component of Green lane depends on (1). Because the fluctuation of the phase is in direct proportion to the multiple number which is used in the case of making reference frequency. The decreasing of power components in high-frequency range depends on (1) and (2).

Table 2–1. *Standard deviationaind confidence limit for random error of position line. (1630-0730)*

Month	Lane	O. poitt	Lower limit	Standard deviation	Upper limit
Jul.	Red	Hakodate	0.18 lane	0.20 lane	0.22 lane
		Kushiro	0.11 lane	0.12 lane	0,13 lane
		Wakkanai	0.12 lane	0.13 lane	0.14 lane
	Green	Hakodate	0.09 lane	0.10 lane	0.11 lane
		Kushiro	0.07 lane	0.08 lane	0.09 lane
		Wakkanai	0.02 lane	0.03 lane	0.03 lane
	Purple	Hakodate	0.16 lane	0.18 lane	0.19 lane
		Kushiro	0.35 lane	0.38 lane	0.41 lane
		Wakkanai	0.22 lane	0.24 lane	0.26 lane
Oct.	Red	Hakodate	0.27 lane	0.29 lane	0.31 lane
		Kusniro	0.12 lane	0.13 lane	0.14 lane
		Wakkanai	0.13 lane	0.14 lane	0.15 lane
	Green	Hakodate	0.10 lane	0.11 lane	0.12 lane
		Kushiro	0.08 lane	0.99 lane	0.10 lane
		Wakkanai	0.03 lane	0.03 lane	0.03 lane
	Purple	Hakodate	0.19 lane	0.21 lane	0.23 lane
		Kushiro	0.40 lane	0.43 lane	0.46 lane
		Wakkanai	0.26 lane	0.28 lane	0.30 lane
Feb.	Red	Hakodate	0.40 lane	0.43 lane	0.46 lane
		Kushiro	0.18 lane	0.20 lane	0.22 lane
		Wakkanai	0.20 lane	0.21 lane	0.23 lane
	Green	Hakodate	0.14 lane	0.16 lane	0.17 lane
		Kushiro	0.13 lane	0.14 lane	0.15 lane
		Wakkanai	0.04 lane	0.05 lane	0.05 lane
	Purple	Hakodate	0.28 laoe	0.31 lane	0.33 lane
		Kushiro	0.55 lane	0.59 lane	0.64 lane
		Wakkanai	0.38 lane	0.41 lane	0.44 lane
May	Red	Hakodate	0.26 lane	0.28 lane	0.30 lane
		Kushiro	0.12 lane	0.13 lane	0.14 lane
		Wakkanai	0.13 lane	0.14 lane	0.15 lane
	Green	Hakodate	0.10 lane	0.11 lane	0.12 lane
		Kushiro	0.08 lane	0.09 lane	0.10 lane
		Wakkanai	0.02 lane	0.03 lane	0.03 lane
	Purple	Hakodate	0.18 lane	0.20 lane	0.22 lane
		Kushiro	0.39 lane	0.42 lane	0.45 lane
		Wakkanai	0.25 lane	0.27 lane	0.29 lane

2-4 Comparison of statistical characteristics of random error series of night time position line between two observational points in the frequency domain

In a common statistical analysis, we use covariance and correlation coefficient in order to examine the linearity between two variables. But it is necessary to

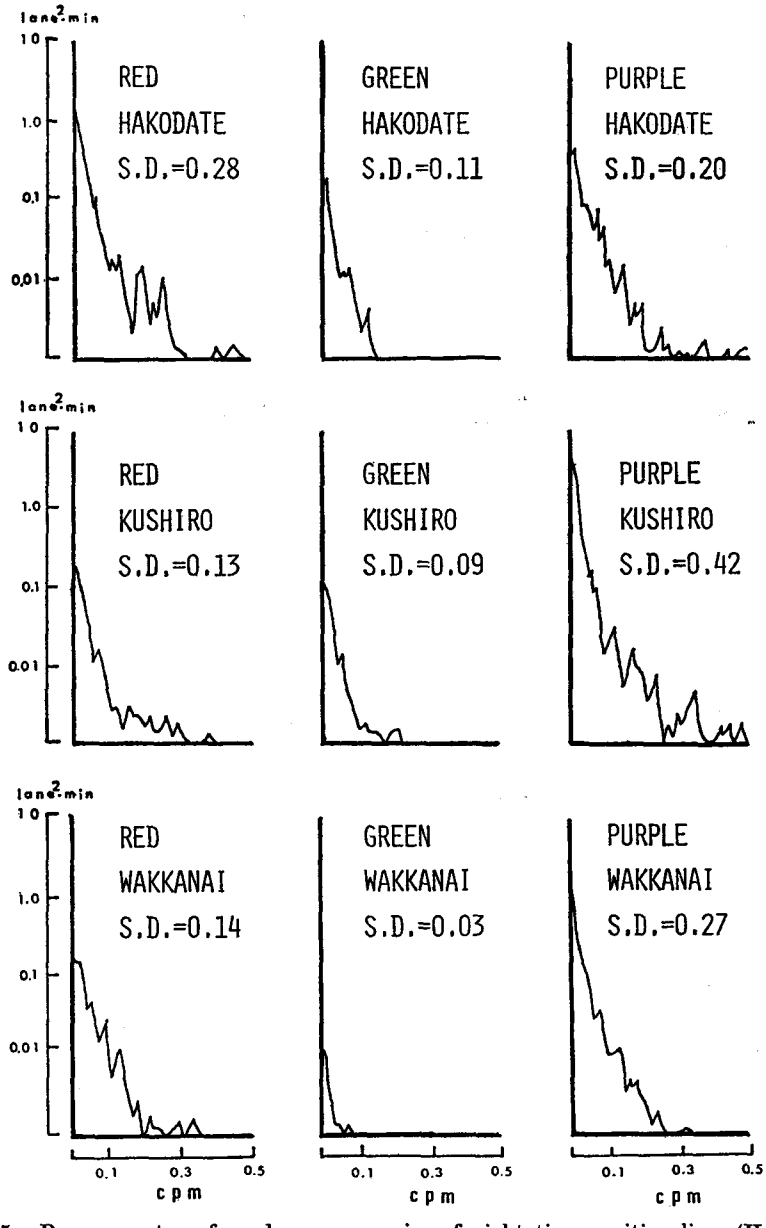

Fig. 2–5. Power spectra of random error series of night time position line. (Hakodate, Kushiro, Wakkanai)

consider the power component in the frequency domain, in the time of detail consideration of random error series of position line for the Decca system. This chapter first serves the imformation of single input-single output linear system

where random error series at one observational point is input and at other observational point is output.

Now given two stationary Gaussian processes $Z_1(s)$ and $Z_2(s)$ which have zero mean, the autocorrelation and crosscorrelation function of random error series of position line between two observational points are given by

$$\begin{aligned} C_{11}(\tau) &= E\{Z_1(s)\, Z_1(s-\tau)\} \\ C_{22}(\tau) &= E\{Z_2(s)\, Z_2(s-\tau)\} \\ C_{21}(\tau) &= E\{Z_2(s)\, Z_1(s-\tau)\} = \int_{-\infty}^{\infty} h(u)\, C_{11}(\tau-u)\, \mathrm{d}u \\ &= h(u)\, C_{11}(\tau) \end{aligned} \qquad (2\text{–}5)$$

where $h(\tau)$ is the impulse response function of this system

Power spectrum and cross spectrum are defined as the Fourier transform of $C_{11}(\tau)$, $C_{22}(\tau)$ and $C_{21}(\tau)$

$$\begin{aligned} P_{11}(f) &= \int_{-\infty}^{\infty} C_{11}(\tau) \exp\{-j\omega\tau\}\, \mathrm{d}\tau \\ P_{22}(f) &= \int_{-\infty}^{\infty} C_{22}(\tau) \exp\{-j\omega\tau\}\, \mathrm{d}\tau \\ P_{21}(f) &= \left[\int_{-\infty}^{\infty} h(u) \exp\{-j\omega u\}\, \mathrm{d}u\right]\left[\int_{-\infty}^{\infty} C_{11}(\tau-u) \exp\{-j\omega(\tau-u)\}\, \mathrm{d}u\right] \\ &= H(f)\, P_{11}(f) \end{aligned} \qquad (2\text{–}6)$$

where $H(f)$ is the frequency response function which is defined as the Fourier transform of $h(\tau)$

The coherency function is given by

$$\gamma^2(f) = \frac{|P_{21}(f)|^2}{P_{22}(f)\, P_{11}(f)} = 1 - \frac{P_{nn}(f)}{P_{22}(f)} \qquad (2\text{–}7)$$

where $P_{nn}(f)$ is a Gaussian process which is independent of the process $Z_1(s)$, and which represents the additive disturbance of an extraneous noise. The coherence function may be thought of as a measure of linear relationship in the sense that the function attains a theoretical maximum unity for all 'f' in a linear system.

Fig. 2–6, Fig. 2–7 and Fig. 2–8 give the results of applications of the above mentioned procedure to observational time series of random error series of position line at three observational points.

(1) *Analysis of the linear relationship of random error series between Hakodate and Kushiro*

(a) Red lane

The gain is about 0.3, and shows a tendency to increase in high-frequency range. The angle of the phase is zero in the ultra-low frequency range and 0.3 CPM, but the

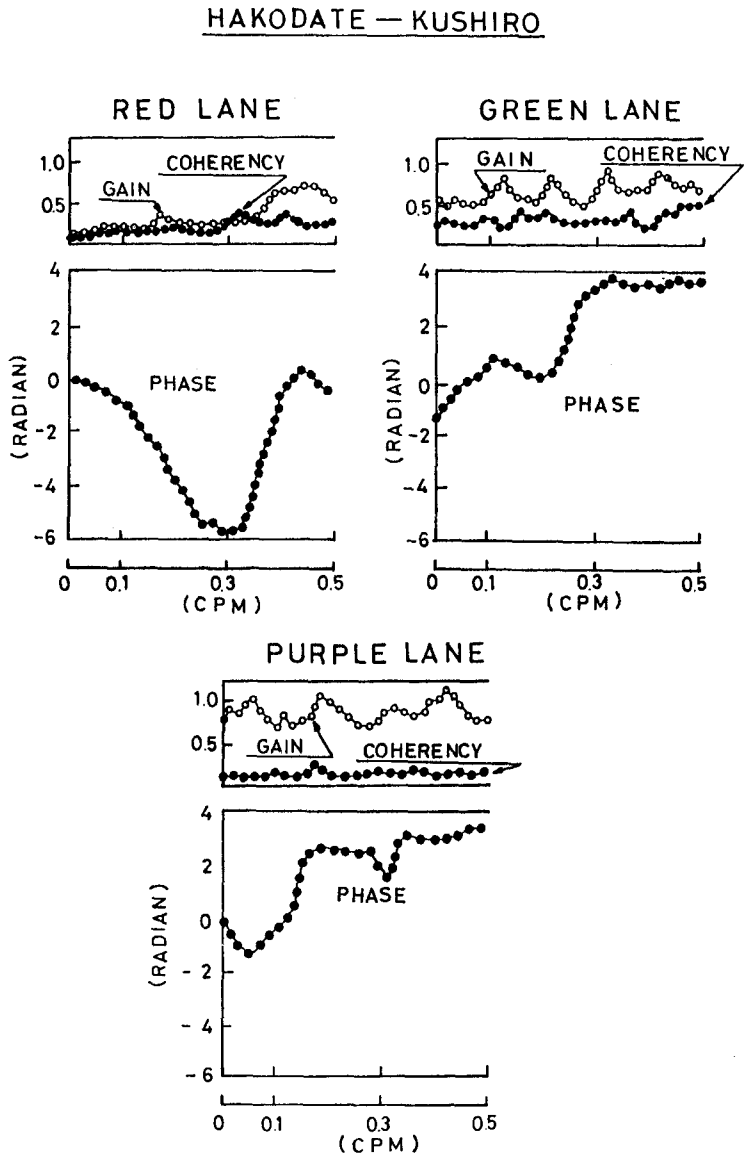

Fig. 2–6. Response characteristics and coherency between Hakodate and Kushiro.

angle of ahead of the phase is 6 radian in another range. That is to say, the variation of random error series of Red lane at Kushiro is behind the one at Hakodate. Red lane has this tendency especially in IF range. Furthermore the coherency which is the measure of a linear relation is low in the whole frequency range, and we can wee that there is a linear dependence between the two.

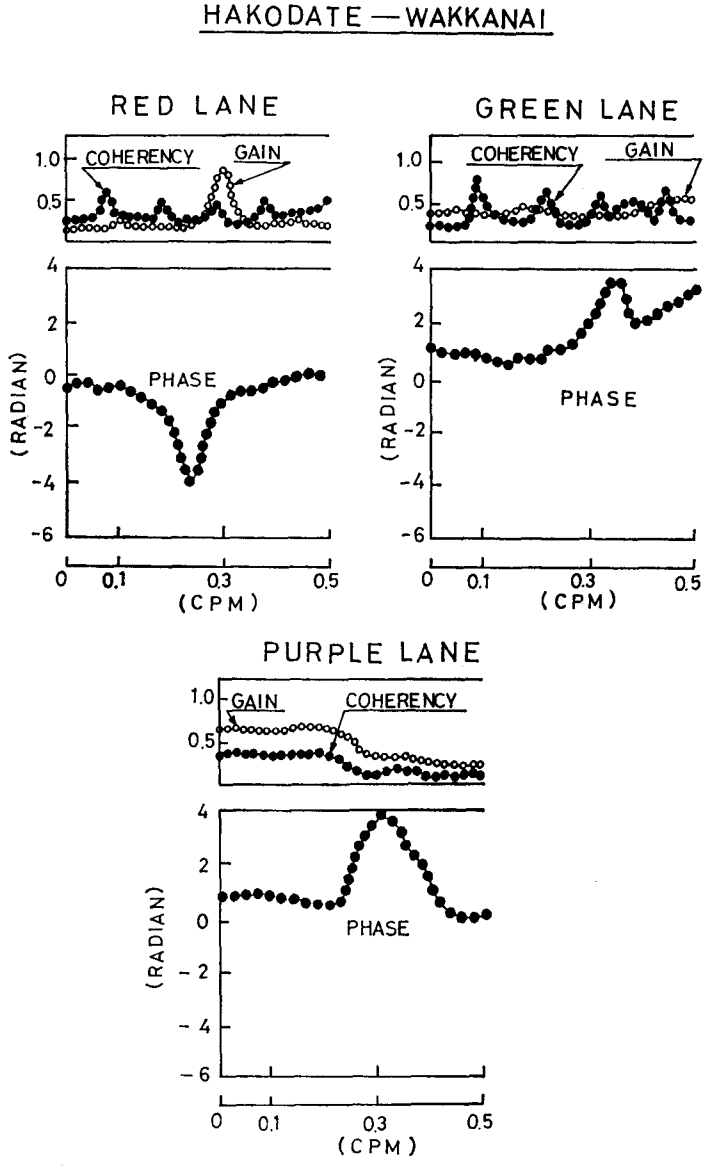

Fig. 2–7. Response characteristics and coherency between Hakodate and Wakkanai.

(b) Green lane

The gain is 0.5 and shows about 0.7 almost-periodically. The angle of ahead of the phase shows a tendency to increase, especially 4 radian from 0.2 CPM to 0.3 CPM. That is to say, the variation of random error series of Green lane at Kushiro

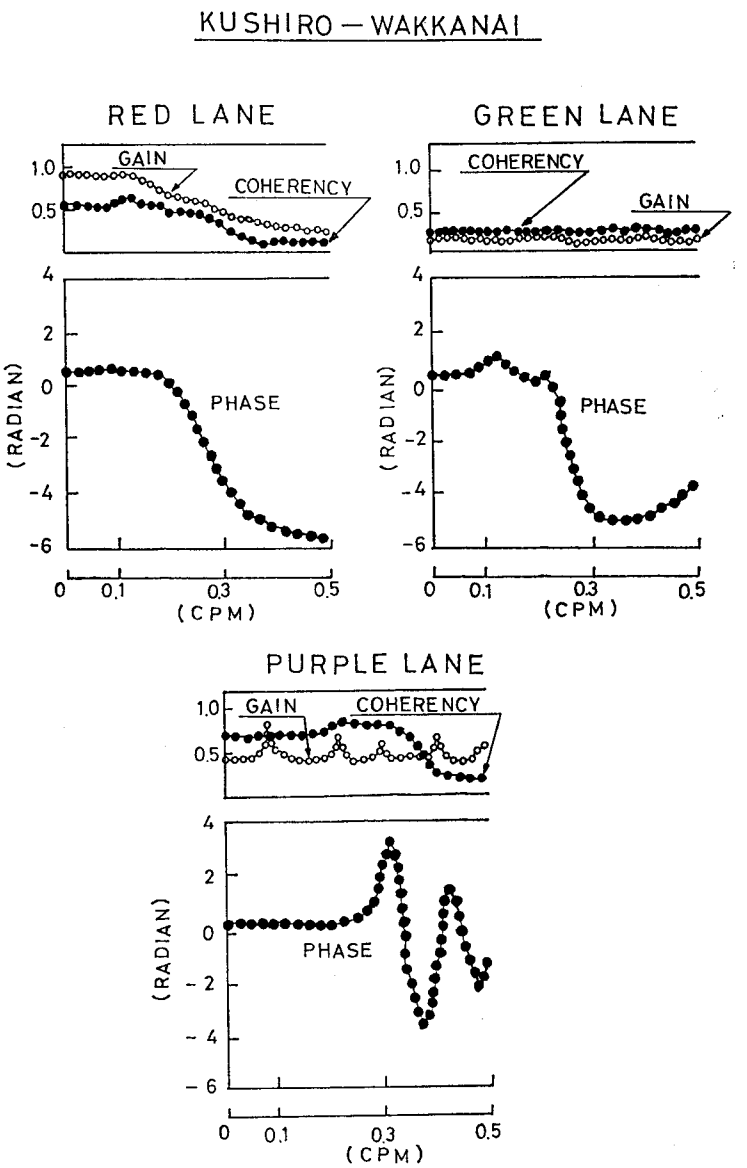

Fig. 2–8. Response characteristics and coherency between Kushiro and Wakkanai.

is ahead of the one at Hakodate. The coherency is low, and we can see that there is a linear dependence between the two.

(c) Purple lane

The gain is 0.7 and shows 1.0 in the ultra-low-frequency range, 0.2 CPM and 0.4 CPM. The angle of lead of the phase is 3 radion with the exception of ultra-

low-frequency range. The variation of ranfom error series of Purple lane at Kushiro is ahead of the one at Hakodate, and this tendency shows especially in high-frequency range. The coherency of Purple lane is extremely low in the whole frequency range, and we can see that there is a linear dependence between the two.

(2) *Analysis of the linear relationship of random error series between Hakodate and Wakkanai*

(a) Red lane

The gain is 0.2 and shows a tendency to increase in 0.3 CPM. We can't see the angle of ahead of the phase, and the angle of lag of the phase is 4 radian in 0.2 CPM and 0.3 CPM. That is to say, we can't see time lag between the variation of random error series of Red lane at Hakodate and at Wakkanai. The coherency of Red lane is low, but we can see 0.6 almost-periodically.

(b) Green lane

The gain is 0.3 and shows a tendency to increase in high-frequency range. The angle of the phase shows a tendency to ahead, especially in high-frequency range. The variation of random error series of Green lane at Wakkanai is ahead of the one at Hakodate, and this tendency shows especially in high-frequency range. The coherency of Green lane is extremely low, but we can see 0.7 almost-periodically.

(c) Purple lane

The gain is 0.6 from ultra-low-frequency range to 0.3 CPM, but is reduced to one-half in high-frequency range. The angle of ahead of the phase is 0.5 radian and especially 3.5 radian in 0.3 CPM and 0.45 CPM. The variation of random error series of Purple lane at Wakkanai is ahead of the one at Hakodate, and this tendency shows especially in IF range. The coherency of Purple lane is 0.5 from ultra-low-frequency range to 0.2 CPM, but gradually decreases as the frequency increases.

(3) *Analysis of the linear relationship of random error series between Kushiro and Wakkanai*

(a) Red lane

The gain is 0.1 from ultra-low-frequency range to 0.1 CPM, and is reduced gradually in high-frequency range. The angle of the phase shows a tendency to be stable, but is 0.6 radian in higher-frequency range. That is to say, the variation of random error series of Red lane at Kushiro is ahead of the one at Wakkanai, and this tendency shows especially in high-frequency range. The coherency of Red lans is 0.5 from ultra-low-frequency range to 0.2 CPM, but gradually reduces in higher-frequency range. We can see that there is a linear dependence between the two, especially in high-frequency range.

(b) Green lane

The gain is 0.1. The angle of the phase shows a tendency to be stable, but is 5 radian of lag in high-frequency range. The variation of random erro series of Green lane at Wakkanai is behind the one at Kushiro, especially in high-frequency range. The coherency of Green lane is extremely low, and we can see that there is a linear dependence between the two.

(c) Purple lane

The gain is 0.4, but we can see 0.6 almost-periodically. The angle of the phase is stable from ultra-low-frequency to high-frequency range. The coherency of Purple lane is high from 0.1 CPM to 0.3 CPM but low in another frequency range.

Putting all results together, it is evident that the random error series of each lane at Hakodate, Kushiro and Wakkanai is linear dependent in the frequency domein.

2-5 The time-constant and the band-width of random error series of position line

When a random error series of position line is stationary and Gaussian process, the autocorrelation function near the straight point is given as

$$C(\tau) = \exp\left(\frac{-\tau^2}{\alpha^2}\right) \tag{2-8}$$

where α is in the time dimension, and the index of the width of correlation for this process.[10)]

Power spectrum is defined as the Fourier transform of $C(\tau)$

$$P(f) = \int_{-\infty}^{\infty} \exp\left\{\frac{-\tau^2}{\alpha^2}\right\} \exp\{-j2\pi f\tau\}\, d\tau \tag{2-9}$$

$$= \frac{\alpha}{2\sqrt{\pi}} \exp\{-\pi^2\alpha^2 f^2\}$$

and the band-width at which the power spectrum reduces one-half (6db) is given as

$$f_e = \frac{0.83}{\alpha\pi} \tag{2-10}$$

where $$\frac{\alpha}{2\sqrt{\pi}} \exp\{-\pi^2\alpha^2 f_e^2\} = \frac{\alpha}{4\sqrt{\pi}}$$

The time-constant τ_0 is the value of τ which is defined by $C(\tau)=e^{-1}$ and the relationship between the time-constant and the band-width is given by

$$f_e = \frac{0.83}{\tau_0\pi} \tag{2-11}$$

Fig. 2-9 give the relationship between the two.

The width of variation for random error series of position line in the time domain can be described bu using the standard deviation. On the other hand, we need an index which describes the statistical characteristics in the frequency domein. It becomes evident that we must pay our attention to the low-frequency range according to the results of section 2-4, and the band-width is the value

corresponding to the estimate of the results of control in the frequency domain in Chapter 3. Fig. 2–10 shows the relationship between the band-width and the atandard deviation of position line, and the standard deviation varies inversely with the increase of the band-width.

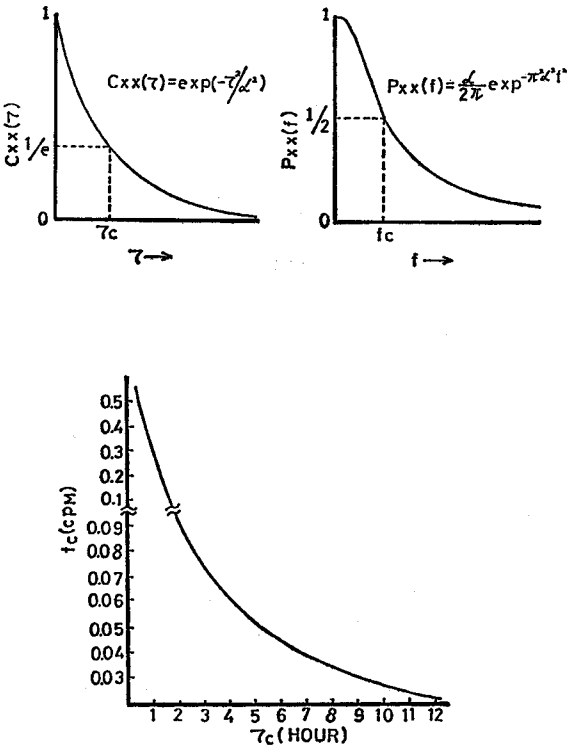

Fig. 2–9. Definition of time-constant (Hour) and band-width (CPM), and relationship between band-width and time-constant.

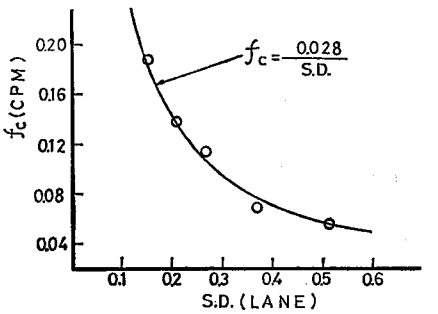

Fig. 2–10. Relationship between band-width (CPM) and standard deviation (Lane).

2-6 The relationship between maxima and slip-lane for random error series of night time position line

The theoretical consideration for the amplitude of maxima of stochastic process first reported by O. Rice and many application have been made.[10)11)12)] In this section, the results of application of this procedure to slip-lane of night time position line is discussed, and the value of the standard deviation in order to hold the slip-lane is decided.

When random error series of position line is stationary and Gaussian process, zero order, second order and fourth order are given by power spectrum $P(\omega)$ such as

$$m_0 = \frac{\alpha(\text{S.D.})^2}{2\sqrt{\pi}} \frac{1}{2} \sqrt{\frac{4\pi}{\alpha}} = \frac{1}{2}(\text{S.D.})^2 \qquad (n=0)$$

$$m_2 = \frac{(\text{S.D.})^2}{2\sqrt{\pi}} \frac{1}{2^2} \sqrt{\left(\frac{4}{\alpha^2}\right)^2 \pi} = \frac{(\text{S.D.})^2}{\alpha^2} \qquad (n=1) \qquad (2\text{–}12)$$

$$m_4 = \frac{(\text{S.D.})^2}{2\sqrt{\pi}} \frac{3}{2^3} \sqrt{\left(\frac{4}{\alpha^2}\right)^5 \pi} = \frac{6(\text{S.D.})^2}{\alpha^4} \qquad (n=2)$$

where

$$m_{2n} = \frac{(\text{S.D.})^2}{2\sqrt{\pi}} \cdot \alpha \cdot \int_{-\infty}^{\infty} \omega^{2n} \exp\left\{-\frac{\alpha^2\omega^2}{4}\right\} d\omega$$

When we substitute m_0, m_2 and m_4 for $\varepsilon^2 = m_0 m_4 - m_0 m_2^2 / m_0 m_4$, we get

$$\varepsilon^2 = \frac{2}{3}, \qquad \varepsilon = 0.82 \qquad (2\text{–}13)$$

From these formulae and results, it is found that the value for the maxima of random error series of night time position line is 0.82. So it is evident that the maxima of this stochastic process represent the Gaussian distribution. Table 2–2

Table 2–2. *Calculated ε and number of heavy monents from power spectra of each lane.*

Lane	O. point	ε	M_0	M_2	M_4	N_0	N_1
Red	Hakodate	0.79	0.078	3.39	20.47	0.59	0.39
	Kushiro	0.82	0.017	2.49	14.01	0.52	0.37
	Wakkanai	0.85	0.019	1.13	5.87	0.51	0.40
Green	Hakodate	0.83	0.012	1.16	11.12	0.63	0.41
	Kushiro	0.82	0.081	5.50	35.00	0.68	0.40
	Wakkanai	0.79	0.001	2.79	17.32	0.63	0.39
Purple	Hakodate	0.83	0.040	1.44	8.33	0.59	0.38
	Kushiro	0.75	0.176	5.73	29.87	0.50	0.36
	Wakkanai	0.78	0.073	0 61	3.73	0.61	0.39

shows the measured mo, m2 and m4 of each lane at Hakodate, Kushiro and Wakkanai by power spectrum. The measured parameter for the maxima of position line equals from 0.75 to 0.85, and it is evident that the maxima for the position line of the Hokkaido Decca chain represent Gaussian distribution. The peak of maxima corresponding to it is above the mean over 1.1·S.D. and 0.8·S.D.

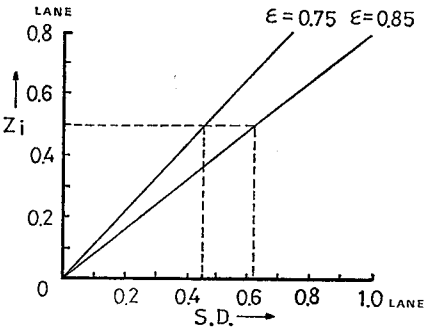

Fig. 22-11. Relationship between maxima (Lane) and standard deviation (Lane).

We have the possibility of slip-lane, when the indication of decometer reduces suddenly at the time of increasing more than 0.5 lane. It has been reported that the range of standard deviation is less than 0.5 lane in Decca tecknical data (no. 203)[5], but it has no theoretical background. So we had better consider the maxima of random error series of position line referring to the possibility of slip-lane at night. In this section an allowable standard deviation by the peak of the distribution of the maxima is described, having an eye on the characteristics of maxima.

Fig. 2-11 shows the relationship between the maxima and the standard deviation at ε=0.75 and ε=0.85. This figure shows the standard deviation of random error series of position line must be kept less than 0.45 lane.

3. Time series analysis between field strength and position line[8]

3-1 Probability density function of the envelope and the phase for composite wave of ground wave plus sky wave[13][14][15][16]

The Decca signal which is distant from the transmitting station is received as a composite wave of constant ground wave plus sky wave scattered from the ionosphere, so the composite wave is given as

$$y(t) = A\cos(\omega_c t+\psi)+b(t) \tag{3-1}$$

Where $b(t)$ is time series of sky wave, which is a narrow band Gaussian process.

The development of (3-1) is given by

$$y(t) = B_c(t)\cos\omega_c t - B_s(t)\sin\omega_c t \tag{3-2}$$

where $B_c(t) = A\cos\psi+b_c(t)$ and $B_s(t) = A\sin\psi+b_s(t)$

$$y(t) = V(t)\cos[\omega_e t + \phi(t)] \tag{3-2}'$$

where $V(t) = [B_c^2(t) + B_s^2(t)]^{1/2}$, $\phi(t) = \tan^{-1}[B_s(t)/B_c(t)]$

In (3-2), $b_c(t)$ and $b_s(t)$ are independent Gaussian random variables, which have zero mean and variance δ_b^2.

So the joint probability density function $P(B_c t, B_s t, \psi)$ and $P(V_t, \phi_t, \psi)$ are given by

$$P(B_{ct}, B_{st}, \psi) = \frac{1}{2\sqrt{\pi}} \frac{\exp\left[-\frac{(B_{ct}-A\cos\psi)^2}{2\delta_b^2}\right]\exp\left[-\frac{(B_{st}-A\sin\psi)^2}{2\delta_b^2}\right]}{(2\pi\delta_b^2)^{1/2}}$$

$$= \frac{1}{4\pi^2\delta_b^2}\exp\left[-\frac{B_{ct}^2+B_{st}^2-2A(B_{ct}\cos\psi+B_{st}\sin\psi)}{2\delta_b^2}\right]$$

$$(0 \leq \psi \leq 2\pi) \tag{3-3}$$

$$P(V_t, \phi_t, \psi) = \frac{V_t}{4\pi^2\delta_b^2}\exp\left[-\frac{V_t^2+V^2-2AV_t\cos(\phi_t-\psi)}{2\delta_b^2}\right];$$

$$V_t \geq 0,\ \phi_t \geq 0,\ \psi \leq 2$$

$$= 0\ ; \qquad \text{other}$$

The probability distribution function of $V(t)$ is given by integrating from zero to 2π with respect to ψ and from -2π to $2\pi-\psi$ with respect to ϕ_t

$$P(V_t) = \frac{V_t}{\delta_b^2}\exp\left(-\frac{V_t^2+A^2}{2\delta_b^2}\right)\frac{1}{2\pi}\int_0^{2\pi} d\psi \frac{1}{2\pi}\int_{-\psi}^{2\pi-\psi}\exp\left(\frac{AV_t}{\delta_b^2}\cos\theta\right)d\theta \tag{3-4}$$

Where $\theta = \phi_t - \psi$, $V_t \geq 0$

In (3-4), the exponential factor $\exp(AV_t\cos\theta/\delta_b^2)$ is the periodic function of θ, so we have (3-5) integrating from zero to 2π with θ.

$$P(V_t) = \frac{V_t}{\delta_b^2}\exp\left(-\frac{V_t^2+A^2}{2\delta_b^2}\right)I_0\left(\frac{AV_t}{\delta_b^2}\right);\quad V_t \geq 0$$

$$= 0\ ; \qquad V_t < 0 \tag{3-5}$$

for a particular case, (3-5) is replaced by

$$P(V_t) = \frac{1}{\delta_x}\left(\frac{V_t}{2\pi A}\right)^{1/2}\exp\left[-\frac{(V_t-A)^2}{2\delta_b^2}\right] \tag{3-6}$$

where $AV_t \gg \delta_b^2$

From these formulae, we get two important results.

(1) The field strength of the Decca signal which is transmitting near the Decca station at night is Gaussian distributed.
(2) The field strength of the Decca signal which is transmitting far from the Decca station at night is Laylie distributed.

The joint probability density function $P(\phi_t, \psi)$ is given by integrating (3–6) from zero to infinite with Vt

$$P(\phi_t, \psi) = \frac{1}{4\pi^2\delta_b^2} \int_0^\infty V_t \exp\left[-\frac{V_t^2+A^2-2AV_t\cos(\phi_t-\psi)}{2\delta_b^2}\right] dV_t \qquad (3\text{–}7)$$

let $\theta = \phi_t - \psi$

$$P(\phi_t, \psi) = \frac{1}{4\pi^2\delta_b^2} \exp\left(-\frac{A^2\sin^2\theta}{2\delta_b^2}\right) \int_0^\infty V_t \exp\left[-\frac{(V_t-A\cos\theta)^2}{2\delta_b^2}\right] dV_t \qquad (3\text{–}8)$$

Approximately, we have

$$P(\phi_t, \psi) = \frac{A\cos(\phi_t-\psi)}{(2\pi)^{3/2}\delta_b} \exp\left[-\frac{A^2\sin^2(\phi_t-\psi)}{2\delta_b^2}\right] \qquad (3\text{–}9)$$

where $0 < \phi_t, \quad \phi \leq 2\pi$

K.A. Norton theorized on the assumption of dependency between the amplitude and the phase of a composite wave.[17][18] According to these theories, The Maritime Safety Agency analyzed the propagation characteristics of the Hokkaido Decca chain.[5] But it is evident from (3–3), (3–5) abd (3–9) that the amplitude and the phase are dependent on the assumption that the amplitude and the phase are not random variables but random processes. So we obtain the probability of the setting of two inputs one output linear system where the inputs are the time series of field strength from master and slave stations and the output is the time series of position line. In section 3–2, we consider the frequency response function of this system.

3-2 Frequency response characteristics between the time series of position line and the one of field strength from master and slave stations

Now given the two inputs one output linear system as pictured in the sketch below

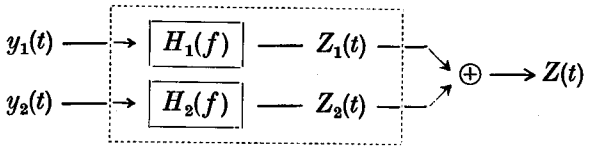

where
$y_1(t)$; the time series of field strength from master station
$y_2(t)$; the time series of field strength from slave station
$Z(t)$; the time series of position line

The frequency response function and cross spectrum and power specrrum are given by

$$\begin{aligned} H(f) &= [H_1(f), H_2(f)] \\ P_{yx}(f) &= [P_{1x}(f), P_{2x}(f)] \\ P_{yy}(f) &= \begin{bmatrix} P_{11}(f) & P_{12}(f) \\ P_{21}(f) & P_{22}(f) \end{bmatrix} \end{aligned} \tag{3-10}$$

When the two inputs are correlated, the general results for the correlated input is written as the matrix equation

$$P_{ix}(f) = \sum_{j=1}^{2} H_j(f)\, P_{ij}(f) \qquad (i = 1, 2) \tag{3-11}$$

where $P_{y_i x}(f) = P_{ix}(f)$

This is equivalent to

$$\begin{bmatrix} P_{1x}(f) \\ P_{2x}(f) \end{bmatrix} = \begin{bmatrix} P_{11}(f) & P_{12}(f) \\ P_{21}(f) & P_{22}(f) \end{bmatrix} \begin{bmatrix} H_1(f) \\ H_2(f) \end{bmatrix} \tag{3-12}$$

and its solution is

$$\begin{bmatrix} H_1(f) \\ H_2(f) \end{bmatrix} = \begin{bmatrix} P_{22}(f)/\Delta & -P_{12}(f)/\Delta \\ -P_{21}(f)/\Delta & P_{11}(f)/\Delta \end{bmatrix} \begin{bmatrix} P_{1x}(f) \\ P_{2x}(f) \end{bmatrix} \tag{3-13}$$

where Δ is the determinant of $P_{xx}(f)$ which is

$$\Delta = P_{11}(f)\, P_{22}(f) - |P_{12}(f)|^2$$

The results are[19)20)21)]

$$\begin{aligned} H_1(f) &= \frac{P_{22}(f)\, P_{1x}(f) - P_{12}(f)\, P_{2x}(f)}{P_{11}(f)\, P_{22}(f) - |P_{12}(f)|^2} \\ &= \frac{P_{1x}(f)\left[1 - \dfrac{P_{12}(f)\, P_{2x}(f)}{P_{22}(f)\, P_{1x}(f)}\right]}{P_{11}(f)\,[1 - \gamma^2_{12}(f)]} \\ H_2(f) &= \frac{P_{11}(f)\, P_{2x}(f) - P_{21}(f)\, P_{1x}(f)}{P_{11}(f)\, P_{22}(f) - |P_{12}(f)|^2} \\ &= \frac{P_{2x}(f)\left[1 - \dfrac{P_{21}(f)\, P_{1x}(f)}{P_{11}(f)\, P_{2x}(f)}\right]}{P_{22}(f)\,[1 - \gamma^2_{12}(f)]} \end{aligned} \tag{3-14}$$

Where $\gamma^2_{12}(f) = |P_{12}(f)|^2 / P_{11}(f)\, P_{22}(f)$

The partial coherency function which is a partial correlation coeffcient between the time series of field strength from master station and the one of position line, taking account of the time series of field strength from slava station, can be defined as

$$\text{Partial coherency } \gamma^2_{1s\cdot 2}(f) = \frac{|P_{is\cdot 2}(f)|^2}{P_{2s\cdot 2}(f)\,P_{11\cdot 2}(f)}$$

$$= \frac{\left[P_{1s}(f) - \frac{P_{2s}(f)\,P_{12}(f)}{P_{22}(f)}\right]\left[P_{s1}(f) - \frac{P_{ss}(f)\,P_{21}(f)}{P_{22}(f)}\right]}{\left[P_{ss}(f) - \frac{|P_{2s}(f)|^2}{P_{22}(f)}\right]\left[P_{11}(f) - \frac{|P_{12}(f)|^2}{P_{22}(f)}\right]} \qquad (3\text{–}15)$$

The partial coherency function which is a partial correlation coefficient between the time series of field strength from slave station and the one of position line, taking account of the time series of field strength from master station, can be defined as

$$\text{Partial coherency } \gamma^2_{2s\cdot 1}(f) = \frac{|P_{2s\cdot 1}(f)|^2}{P_{ss\cdot 1}(f)\,P_{22\cdot 1}(f)}$$

$$= \frac{\left[P_{2s}(f) - \frac{P_{1s}(f)\,P_{12}(f)}{P_{11}(f)}\right]\left[P_{s2}(f) - \frac{P_{ss}(f)\,P_{21}(f)}{P_{11}(f)}\right]}{\left[P_{ss}(f) - \frac{|P_{1s}(f)|^2}{P_{11}(f)}\right]\left[P_{2s}(f) - \frac{|P_{12}(f)|^2}{P_{11}(f)}\right]} \qquad (3\text{–}16)$$

The multiple coherency function which is a multiple correlation coefficient between the time series of field strength from master and slave stations and the one of position line, can be defined as

$$\text{Multiple coherency } \gamma^2_{ys}(f) = \gamma^2_{12\cdot s}(f)$$

$$= \frac{1}{P_{ss}(f)}\,[H_1(f), H_2(f)]\begin{bmatrix} P_{1s}(f)^* \\ P_{2s}(f)^* \end{bmatrix} \qquad (3\text{–}17)$$

Where $P_{s1}(f)=P_{1s}(f)^*$, $P_{s2}(f)=P_{2s}(f)^*$

3-3 The results of time series analysis between field strength, which is transmitting from master and slave stations, and position line

In section 3–1, we describe mathematically that amplitude of composite wave is Lailei distributed when the sky wave is superior to the ground wave and is Gaussian distributed when the ground wave is superior to the sky wave. Fig. 3–1 shows the histogram and probability distribution function of field strength from master and slave stations at night. Field strength from master station (243 Km from Biei), from Red station (382 Km from Akkeshi) and from Green station (415 Km from Wakkanai) are Iailei distributed. On the other hand, field strength from Purple station (71 Km from Oshamambe) is Gaussian distributed.

The purpose of this chapter is not to show the probability distribution function of field strength, but to analyze the frequency response characteristics between the time series of field strength from master and slave stations and the one of position line. On the occasion of analyzing the frequency response characteristics, the normality of input and output variables is necessary condition. So it is necessary

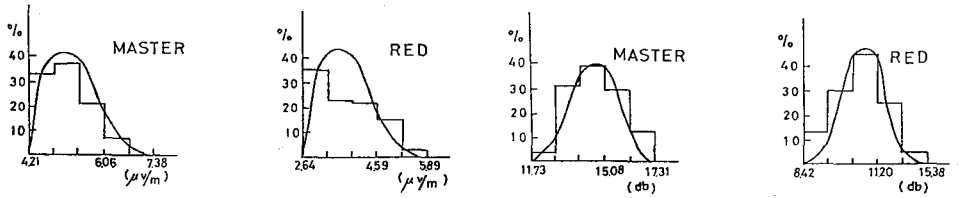

Fig. 3–1. Histogram and probability distribution of position line at night. (Hakodate)

Fig. 3–2. Normalized histogram and probability distribution of position line at night (Hakodate).

for us to normalize variables if they don't satisfy the normality. In this case we adopt the representation of decibels for field strength in order to normalize. Fig. 3–2 shows the histogram and probability distribution function of field strength, which is represented by decibels, from master and slave stations (Red and Green). In Fig. 3–3, we plot the cumulative distribution of these cases of field strength on the Gaussian probability paper, besides the results of χ^2-test of normality. Time series of field strength which is Lailei distributed in 5% level of significance, when we adopt the representation of decibels.

Next we consider the frequency response characteristics between the normalized field strength which is the inputs of this system and position line which is the output of this system, in order to clarify the linear relationship among three random series. One instance out of many, we describe the detail results of Red lane at Hakodate from 7:30 A.M. to 4:30 P.M. December 20 to 21, 1976. At the end of this section, we consider the tendency of frequency response characteristics of all lanes.

Fig. 3–4 shows the observational time series of normalized field strength, which are represented by decibels, from master and slave stations and the one of position line. Fig. 3–5 shows the power spectrum of field strength and position line, the

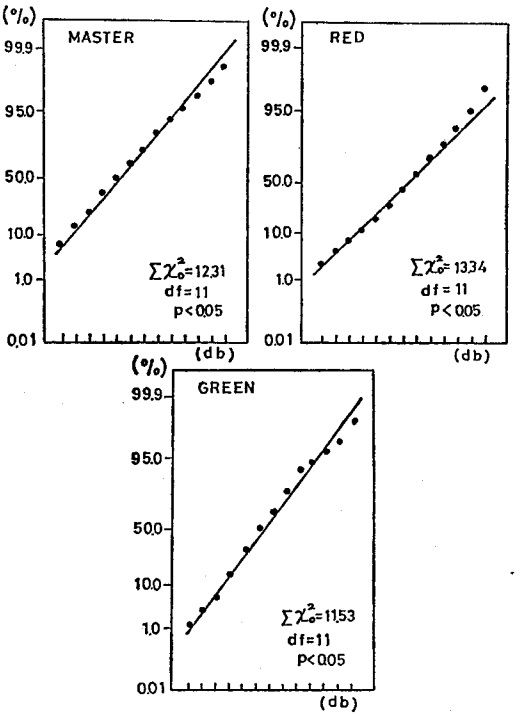

Fig. 3-3. Cumulative distribution of field strength at night. (The records show each distribution representiong the normal distribution)

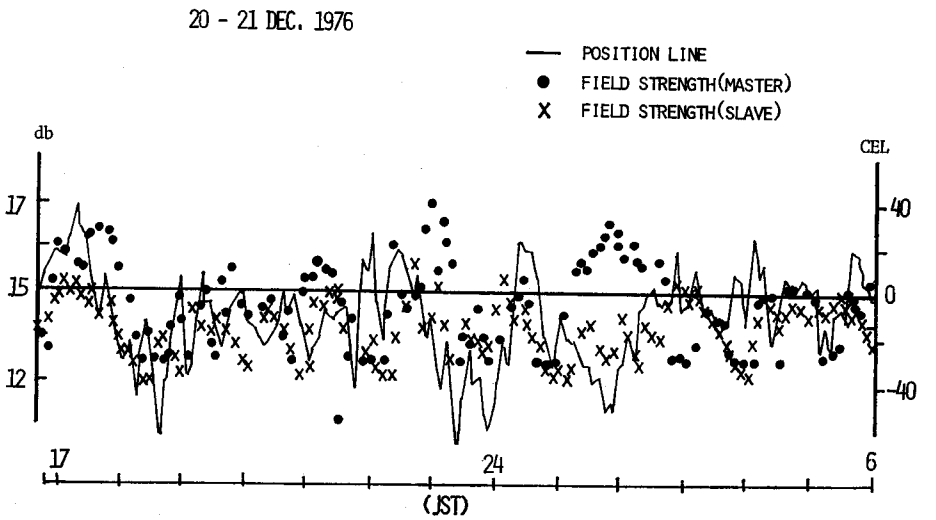

Fig. 3-4. Time history of field strength and position line at Hakodate. (1630–0600)

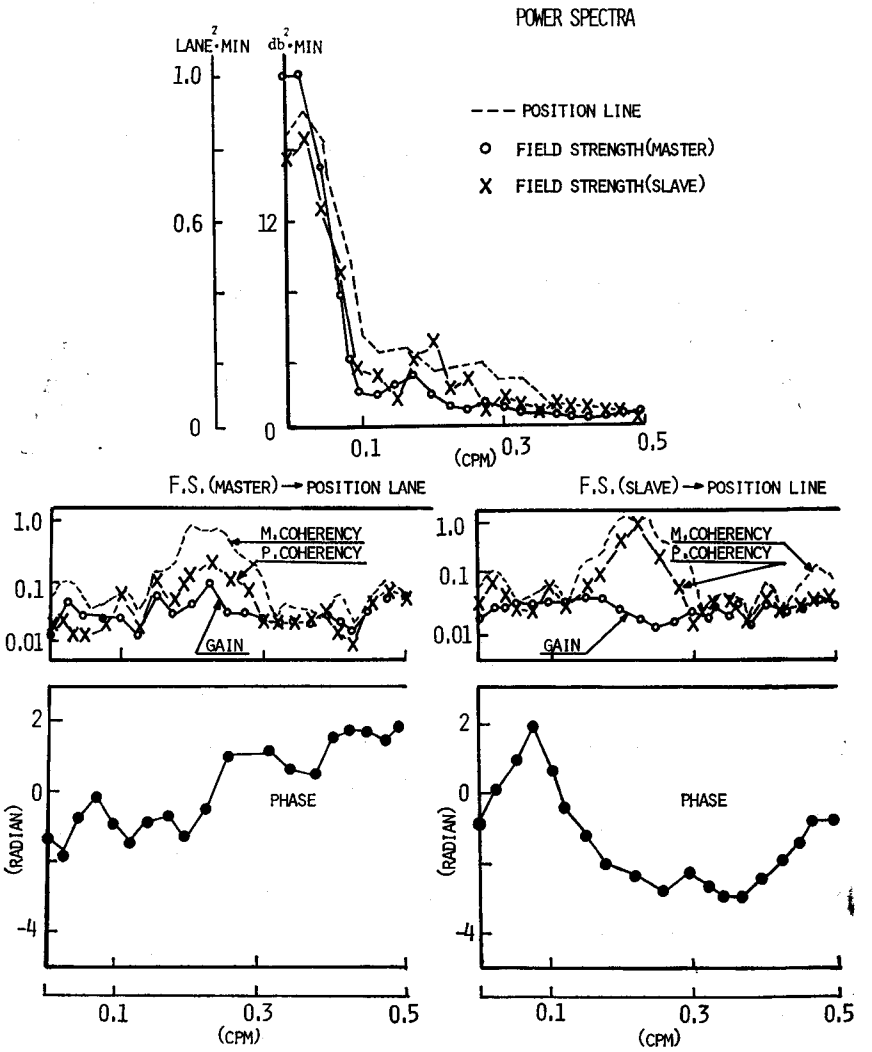

Fig. 3–5. Response characteristics and coherency between field strength and position line.

frequency response function between the time series of field strength from master station and the one of position line, and the frequency response function between the time series of field strength from slave station and the one of position line. According to the shape of the power spectrum, the time series of normalized field strength indicate almost-periodic series which have the greater part of energy in low-frequency range, similar to position line. So we consider the frequency response characteristics especially in low-frequency range.

(1) The frequency response characteristics between the time series of field strength

from master station (Biei) and the one of position line taking into account the time series of field strength from slave station.

The gain is below 0.05, but shows a tendency to increase to 0.3 CPM and 0.5 CPM. The angle of lag of the phase is 1 radian from ultra-low frequency range to 0.3 CPM, but shows a lead in higher-frequency range. That is to say, the variation of time series of field strength from master station is ahead of the one of position line in low-frequency range, but this tencency turns reversively in high-frequency range. The partial coherency is very low, but rather increases to 0.2 CPM and 0.3 CPM.

(2) The frequency response characteristics between the time series of field strength from slave station (Akkeshi) and the one of position line taking into account the time series of field strength from master station.

The gain is below 0.04. The angle of the phase shows a tendency to be delayed of 2 radian with the exception of 0.1 CPM. The frequency response characteristics between the two depend on the frequency range, furthermore its pattern is different from the one between the field strength from master station and position line. The partial coherency is 0.1, but 0.8 from 0.2 CPM to 0.3 CPM.

From these results, it is evident that the linear relationship between the time series of field strength and the one of position line is very low, especially in low-frequency range. We have more knowledge about the statistical characteristics in the frequency domain with analyzing Green lane and Purple lane as follows:

(a) Time series of field strength indicate almost-periodic series which have the greater part of energy in low-frequency range.

(b) The frequency response characteristics depend on the frequency range, and it is impossible to generalize.

(c) The coherency have a tendency to be very low, especially in low frequency range.

(d) The linear relationship between the time series of field strength and the one of position line in low-frequency range is very low, where the power spectrum has greater part of energy.

4. Real time adaptive control for random error series of position line which is observed at a fixed point at night

4-1 Formulation of adaptive control process for random error series which is observed at a fixed point

As we described in the purpose of this study, random error series of position line fluctate randomly throughout the night. So the statistics such as mean and standard deviation don't go far toward reducing the random error of position line. This is because it is necessary for us to forecast and control from past data, to obtain sufficient accuracy of ship's position at fishing. It is natural to consider a model of random error series of position line such as:

(1) We can obtain information at equally spaced time intervals.

(2) The target value of random error series is zero, and there is no loss of generality on account of this condition.

(3) We regard uncontrolled random error series of position line as the true random error series, where these series $Z(s)$ are stationary.

(4) The value of random error series is $Z(s)$-$X(s)$ by making the adjustment $-X$ to true random error series. The value $\varepsilon'(s)$ is equal to the deviation from the target, and we obtaion the fundamental equality

$$\varepsilon'(s) = Z(s) - X(s) \tag{4-1}$$

We now assume the loss is proportional to $\varepsilon'(s)$ by making the adjustment $-X$. The objective of this chapter is to determine the controlled variable $-X$ $(s+1)$ so as to minimize the expected loss $L_{s+1}X(s+1)$.

$$L_{s+1}X(s+1) = E\{\varepsilon^2(s+1)\} = E\{\{Z(s+1)-X(s+1)\}^2\} \tag{4-2}$$

When we prescribe the optimal controlled variable for $-X(s+1)$ at the time $(s+1)$, theories about the optimal controlled variable are given as here below:[24)23)]

In order to determine the optimal controlled variable for $-X(s+1)$, it is necessary for us that $X(s+1)$ be equal to the predicted value $Z_s(1)$ of $Z(s)$, based on $Z(s)$, $Z(s+1)$, $Z(s-2)\cdots$. When we take $X(s+1)$ to be a linear function of Z's

$$X(s+1) = \sum_{j=0}^{\infty} \mu(j)\, Z(s-j) \tag{4-3}$$

and refer to the j's as the predictor weight. Among these controlles variables, X $(s+1)$ which satisfies the condition of (4-2) is equal to optimal linear controlled variable

$$X(s+1) = \sum_{j=0}^{\infty} \hat{\mu}(j)\, Z(s-j) \tag{4-4}$$

According to these theories, an adaptive optimization and control for random error series of position line at a fixed point is equivalent to determine the predicted value from past data.

4-2 Auto regressive model for random error series of night time position line

We assume that random error series $Z(s)$ is a stationary autorevressive process generated by the relation

$$Z(s) = \sum_{m=1}^{M} a(m)\, Z(s-m) + U(s) \tag{4-5}$$

where U's are mutually independent and independently distributed random variables with

$$E\{U(s)\} = 0\,, \qquad E\{U(k)\, U(j)\} = \delta^2 \delta_{kj} \tag{4-6}$$

The mean square value of residual is given by

$$J = E\{U^2(s)\} = E\left\{\left|Z(s) - \sum_{m=1}^{M} a(m)\, Z(s-m)\right|^2\right\}$$

$$= C_{zz}(0) - 2\sum_{m=1}^{M} a(m)\, C_{zz}(m) + \sum_{l=1}^{M}\sum_{m=1}^{M} a(l)\, a(m)\, C_{zz}(m-l) \tag{4-7}$$

from the simultaneous equation of m-th degree, we get the following representation

$$\hat{C}\hat{a} = c \tag{4–8}$$

where

$$C = \begin{pmatrix} c_0, c_1, c_2, \cdots, c_{M-1} \\ c_1, c_2, c_3, \cdots, c_{M-2} \\ \vdots \quad \ddots \quad \vdots \\ c_{M-1}, c_{M-2}, \cdots, c_M \end{pmatrix}, \quad \hat{a} = \begin{pmatrix} a_1 \\ a_2 \\ \vdots \\ a_M \end{pmatrix}, \quad c = \begin{pmatrix} c_1 \\ c_2 \\ \vdots \\ c_M \end{pmatrix}$$

and by taking account the relation

$$J = C_0 - \hat{a}'c \tag{4–9}$$

we get

$$\hat{a} = \hat{C}^{-1}c \tag{4–10}$$

For the computational procedure of $a_M(m)$ and $J(M)$, we have the following recursive realtions[25)26)]

$$\begin{aligned} &a_1(1) = \hat{c}_1/\hat{c}_0 \\ &J(1) = (\hat{c}_0^2 - \hat{c}_1^2)/\hat{c}_0 \\ &\hat{a}_{M+1}(M+1) = \{\hat{c}_{M+1} - (\hat{a}_M(M)c_1 + \cdots + \hat{a}_1(M)\hat{c}_M)\}/J(M) \\ &\hat{a}_i(M+1) = \hat{a}_i(M) - \hat{a}_{M+1}(M+1)\,\hat{a}_{M+1-i}(M), \qquad i = 1, 2, \cdots, M \\ &J(M+1) = J(M)\{1 - (\hat{a}_{M+1}(M+1))^2\} \end{aligned} \tag{4–11}$$

When we secide the degree of autoregressive model of our system, we use the final prediction error (*FPE*) which is defined as the mean square of the predictor

$$FPE(M) = \left(1 + \frac{M+1}{n}\right)\left(1 - \frac{M+1}{n}\right)\delta^2(M) \tag{4–12}$$

Where $\delta^2(M)$ is the estimation of $C_{uu}(0)$

4-3 Auto regressive prediction for random error series of night time position line

When we predict the random error series by the linear combination of the previous setting of order M, the auto regressive prediction is given by

$$\hat{Z}(s) = \sum_{m=1}^{M} a(m)\,Z(s-m) \tag{4–13}$$

and the prediction error is given by

$$\varepsilon'(s) = Z(s) - \hat{Z}(s) = (a_1 - \hat{a}_1)\,Z(s-1) + \cdots + (a_M - \hat{a}_M)\,Z(s-M) + u(s) \tag{4–14}$$

$$E\{\varepsilon'^2(s)\} = \delta^2 + \left\{(a_1 - \hat{a}_1), \cdots (a_M - \hat{a}_M)\,C \begin{pmatrix} a_1 - \hat{a}_1 \\ \vdots \\ a_M - \hat{a}_M \end{pmatrix}\right\} \tag{4–15}$$

By using these relations and the fact that C is the positvie constant vector, it can be shown that the best linear prediction value is given by

$$\hat{Z}(s) = \sum_{m=1}^{M} a(m)\, Z(s-m) \tag{4-16}$$

Where $a_1-a_1=0, \cdots a_M-a_M=0$

(4–16) is equal to (4–13), and the best linear prediction value of auto regressive process is equal to predict by computing the inertial behavior of this system, taking into account the parameter $a_1, a_2, \cdots, a_M$.

The index for the accuracy of prediction is reported as the nondimensional value of mean square value of prediction error

$$\epsilon^2 = \frac{FPE(M)}{\hat{c}(0)} \tag{4-17}$$

where $\hat{c}(0) = E\{Z^2\} = C_{zz}(0)$

But ϵ^2 is inappropriate for our study, because of time lag between the time series for modeling and the one of prediction. we define the estimation function of our study as

$$\varepsilon = \sqrt{\frac{E\{(Z-X)^2\}}{E\{Z^2\}}} = \sqrt{\frac{C_{\varepsilon'\varepsilon'}(0)}{C_{zz}(0)}} = \frac{\delta_{\varepsilon'}}{\delta_z} \tag{4-18}$$

where $C_{zz}(0)$ is equal to the variance of controlled random error series
$C_{\varepsilon'\varepsilon}(0)$ is equal to the variance of prediction error

4-4 The scheme of adaptive control for random error series of night time position line at a fixed point by monitoring method

$E\{Z(s)\}$ at a fixed point is constant, so it satisfies the condition of 4–1–(2). This section describes the concrete scheme of adaptive control for random error series of night time position line at a fixed point by the monitoring method.

(1) The prediction and control for random error series at a fixed point is done by the auto regressive prediction with the aid of a previous auto regressive model at the monitoring point.

(2) Random error series of night time position line is the stationary auto regressive process of order M generated by the relation

$$Z(s) = \sum_{m=1}^{M} a(m)\, Z(s-m) + U(s)$$

(3) The expected loss by making the adjustment $-X(s+1)$ at the time $(s+1)$ is given by

$$E\{\{Z(S+1)-\hat{X}(s+1)\}^2\}$$

and the estimation function of our study is given by the relation

$$\varepsilon = \sqrt{C_{\varepsilon'\varepsilon'}(0)/C_{zz}(0)}$$

(4) We obtain the optimal linear controlled variable at the time $(S+1)$ by the relation

$$X(s+1) = \sum_{m=1}^{M} a(m)\, Z(s-m)$$

(5) The purpose of this control process is to determine the optimal controlled variable $X(s+1)$ at a fixed point as the linear function of the previous Z's with the aid of the previous auto regressive model at the monitoring point, in the sense of minimizing the expected loss.

The control process which satisfies the condition from (1) to (5) can be described completely by the parameter $a_1, a_2, a_3, \cdots, a_M$.

4-5 The relationship between the estimation function and error ellipse

We assume that the error of two position lines X and Y whose angle of cut is φ are Gaussian distributed. If we put those standard deviations as δ_X, and δ_Y, as to any point $A(X, Y)$, the probability of the axis of absicissas to show the true position being between X and $X+dX$ is $\frac{1}{\sqrt{2\pi}\,\delta_X} \exp\left(\frac{X^2 \sin^2\varphi}{2\delta_X{}^2}\right) \mathrm{d}X \sin\varphi$, and the probability of the axis of the ordinates being between Y and $\mathrm{d}Y$ is $\frac{1}{\sqrt{2\pi}\,\delta_Y} \exp\left(-\frac{Y^2 \sin^2\varphi}{2\delta_Y{}^2}\right) \mathrm{d}Y \sin\varphi$.

Therefore, the probability of a ship's position being within the parallelogram overlapped by two fine bands is expressed as follows by the product of both

$$P(X, Y) = \frac{\sin\varphi}{2\pi\delta_X\delta_Y} \exp\left\{-\sin^2\varphi\left(\frac{Y^2}{2\delta_X{}^2} + \frac{X^2}{2\delta_Y{}^2}\right)\right\} \mathrm{d}X\, \mathrm{d}Y \sin\varphi \quad (4\text{–}19)$$

In the probability, as $\mathrm{d}X\mathrm{d}Y\sin\varphi$ is the area of this very small parallelogram, the coefficient $\frac{\sin\varphi}{2\pi\delta_X\delta_Y} \exp\left\{-\sin^2\varphi\left(\frac{Y^2}{2\delta_X{}^2} + \frac{X^2}{2\delta_Y{}^2}\right)\right\}$ is a probability density function in simultanious distributions. Therefore, the locus of a point where the value of the function comes to the equality is expressed by

$$\sin^2\varphi\left(\frac{Y^2}{2\delta_X{}^2} + \frac{X^2}{2\delta_Y{}^2}\right) = \text{const.} \quad (4\text{–}20)$$

and transforming this equation, we get

$$\frac{Y^2}{\sqrt{2c}\,\delta_X{}^2 \operatorname{cosec}\varphi} + \frac{X^2}{\sqrt{2c}\,\delta_Y{}^2 \operatorname{cosec}\varphi} = 1 \quad (4\text{–}21)$$

From equation (4–21), each conjugate semidiameter (aX, aY), and the area of the ellipse S are given by

$$\begin{aligned} a_x &= \sqrt{2c}\,\delta_X \operatorname{cosec}\varphi \\ a_y &= \sqrt{2c}\,\delta_Y \operatorname{cosec}\varphi \\ S &= 2\pi\delta_X\delta_Y \operatorname{cosec}\varphi \end{aligned} \tag{4–22}$$

Where $c = \log_e\left(1 - \dfrac{1}{1-P}\right)$

Now, if P equal to 0.95, we have approximately

$$\begin{aligned} a_x &= 2.44777\delta_X \operatorname{cosec}\varphi \\ a_Y &= 2.4477\delta_Y \operatorname{cosec}\varphi \\ S &= 18.823\delta_X\delta_Y \operatorname{cosec}\varphi \end{aligned} \tag{4–23}$$

The error of controlled position line X^* and Y^* satisfies these equation, we get

$$\begin{aligned} a_x^* &= 2.4477\delta_X^* \operatorname{cosec}\varphi \\ a_y^* &= 2.4477\delta_Y^* \operatorname{cosec}\varphi \\ S^* &= 18.823\delta_X^*\delta_Y^* \operatorname{cosec}\varphi \end{aligned} \tag{4–24}$$

from (4–18), we get

$$\begin{aligned} \delta_X^* &= \varepsilon_X\delta_X \\ \delta_Y^* &= \varepsilon_Y\delta_Y \end{aligned} \tag{4–25}$$

Fig. 4–1 shows the relationship between position line and the estimation function such as

$$\begin{aligned} \frac{a_x^*}{a_x} &= \varepsilon_x \\ \frac{a_y^*}{a_y} &= \varepsilon_Y \\ \frac{S^*}{S} &= \varepsilon_X\varepsilon_Y \end{aligned} \tag{4–26}$$

By the realtion of (4–26), it is evident the controlled conjugate semidiameter (a_x^*, a_y^*) shows a decrease of (ε_X, ε_Y) and the area of the controlled ellipse (S^*) shows a decrease of (ε_X, ε_Y) compared with the uncontrolled ellipse (Fig. 4–2).

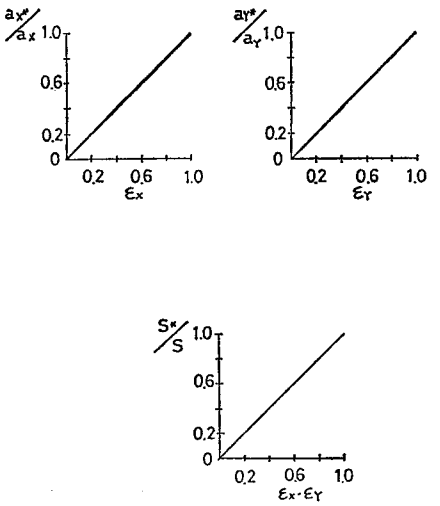

Fig. 4–1. Relationship between a_X^*/a_X and ε_x, a_y^*/a_y and ε_y, S^*/S and ε_x, ε_y.

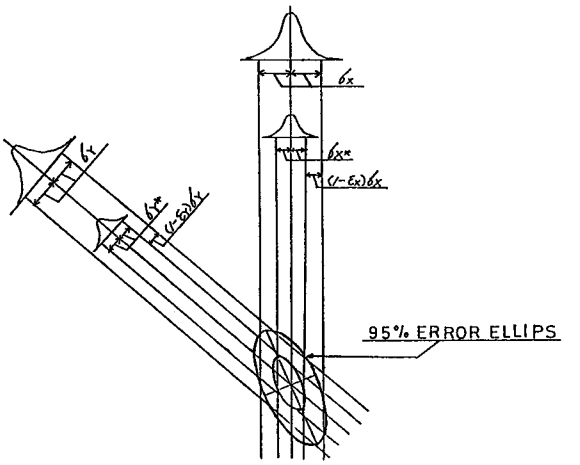

Fig. 4–2. Geometry for 95% error ellipse of observational data and controlled one.

4-6 The ideal frequency response function on the occasion of the estimation for the results of real time adaptive control in the frequency domain

In section 4–1, we discussed the formation of real time adaptive control for random error series by the monitoring method. Also it is necessary for us to estimate the results of control in the frequency domain. Because the random error series of night time position line have the greater part of energy in low-frequency range, we can't accomplish our object if the real time adaptive control isn't effective especially in low-frequency range. In this section, we introduce the ideal frequency response function of adaptive control by means of setting the linear system where the observational random error series of night time position line is input and the auto regressive prediction value of the same is output.

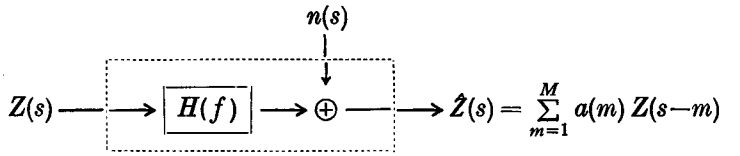

Where $Z(s)$; auto regressive prediction value
$Z(s)$; observational random error series of night time position line

Now given two stationaly Gaussian processes $Z(s)$ and $\hat{Z}(s)$ which have zero mean, the frequency response function of this system is given by

$$H(f) = \frac{P_{zz}(f)}{P_{z\hat{z}}(f)} = |H(f)|\, e^{j\theta(f)} \qquad (4\text{–}27)$$

When the adaptive control is done completely in the whole frequency range, the gain and the phase are given by

$$\begin{aligned} |H(f)| &= 1.0 \\ \theta(f) &= 0.0 \end{aligned} \tag{4-28}$$

By taking into account the condition that the auto regressive prediction takes with time lag necessarily, we get

$$\begin{aligned} |H(f)| &= 1.0 \\ \theta(f) &= -2\pi\tau f \end{aligned} \tag{4-29}$$

Where τ is time lag

The coherency function is given by

$$\gamma^2(f) = 1 - \frac{P_{nn}(f)}{P_{zz}(f)} \tag{4-30}$$

When the auto regressive prediction value consists of a linear combination of observational value completely, we get

$$\gamma^2(f) = 1.0 \tag{4-31}$$

Where $P_{nn}(f)$ equal to 0.0 in the whole frequency range.

From (4-29) to (4-31), it is evident that the ideal $|H(f)|$ and $\gamma^2(f)$ are eual to 1.0 in the whole frequency range, and the gradient $-2\pi\tau(f)$ of the phase is as small as possible on the occasion of the estimation for the results of the real time adaptive control in the frequency domain.

4-7 The results of adaptive control for random error series of night time position line at a fixed point by monitoring method

(1) *The results of Red and Green lanes at Rishiri by using the Auto regressive model at Wakkanai which is the monitoring point*

The auto regressive model of Red lane and Green lane at Wakkanai is given by

$$\begin{aligned} Z_r(s) = {} & 1.03882Z_r(s-1) - 0.16773Z_r(s-2) + 0.01971Z_r(s-3) \\ & - 0.05874Z_r(s-4) - 0.00386Z_r(s-5) + 0.13075Z_r(s-6) \\ & - 0.08172Z_r(s-7) - U_r(s) \\ Z_p(s) = {} & 1.16811Z_p(s-1) - 0.28528Z_p(s-2) + 0.00468Z_p(s-3) \\ & + 0.06721Z_p(s-4) - 0.04061Z_p(s-5) + 0.05393Z_p(s-5) \\ & - 0.01684Z_p(s-7) + 0.10626Z_p(s-8) + U_p(s) \end{aligned}$$

The linear optimal controlled value is given by the auto regressive prediction with the aid of the above auto regressive model. Fig. 4-3 and Fig. 4-4 show the

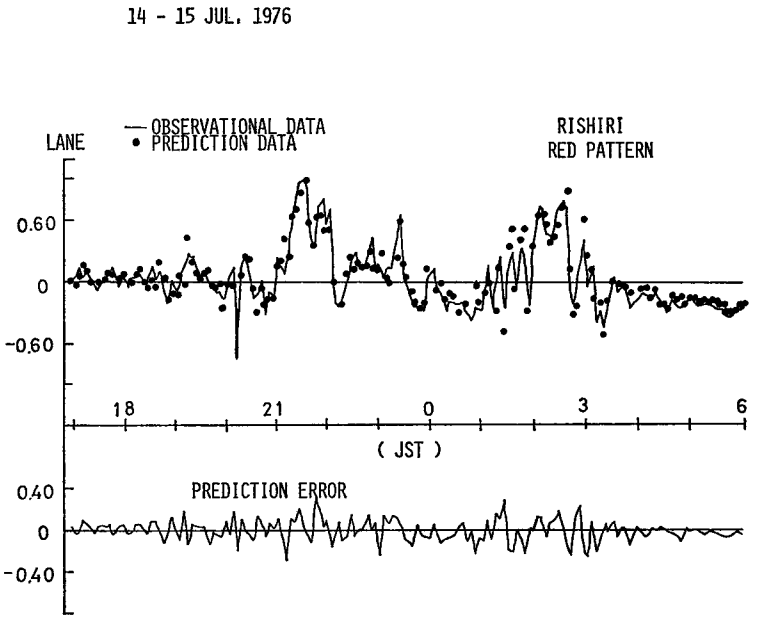

Fig. 4–3. Time history of observational position line, prediction data and prediction error. (1630–0600)

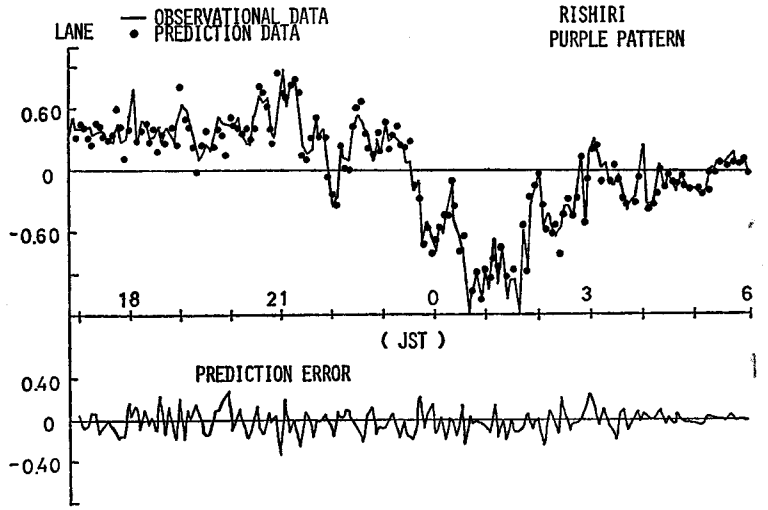

Fig. 4–4. Time history of observational position line, prediction data and prediction error. (1630–0600)

observational random error series, the auto regressive prediction series and the prediction error series of Red and Green lanes July 15–16, 1976. The standard deviation of prediction error of Red lane becomes 0.14 lane and the one of Purple lane becomes 0.13 lane though the standard deviation of observational random error series of Red lane is 0.33 lane and the one of Purple lane is 0.49 lane. This fact shows that the estimation function ε_r, ε_p is equal to 0.43, 0.27 and the variation of random error series of night time position line at Rishiri is reduced to one-half and one-third.

Fig. 4–5 and Fig. 4–6 show the power spectrum and frequency response function at Rishiri. Though the power spectrum of observational data has the greater part of energy in low-frequency range, the one of prediction error equally has small

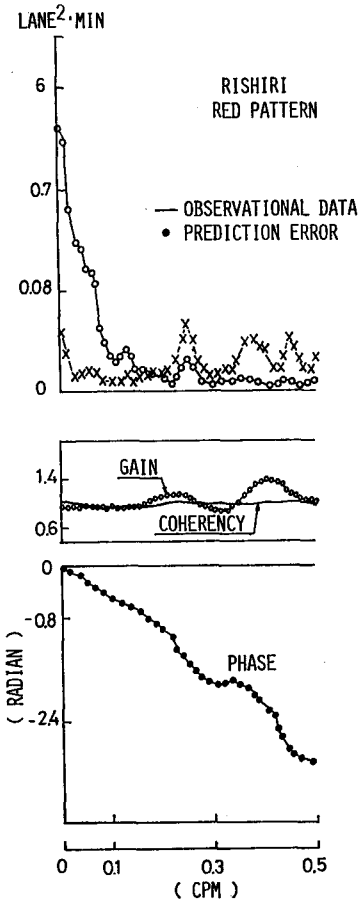

Fig. 4–5. Power spectra, response characteristics and coherency between observational data and prediction data.

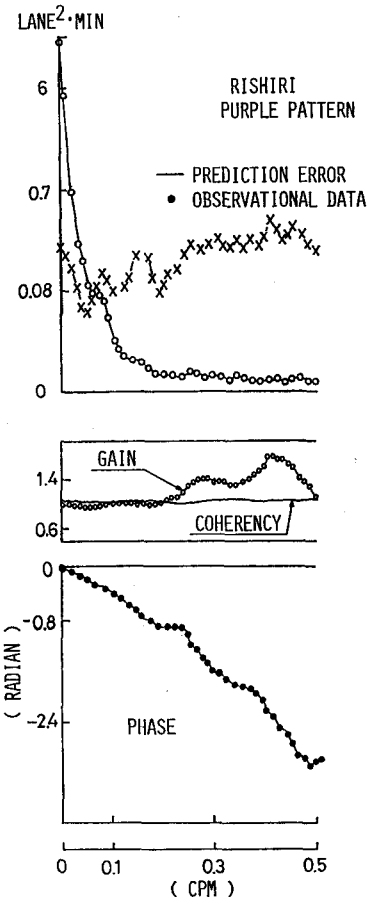

Fig. 4–6. Power spectra, response characteristics and coherency between observational data and prediction data.

energy through the whole frequency range. So it is evident that the variation of random error series in low-frequency range where the power spectrum has the greater part of energy is eliminated completely. The coherency is 0.98 in the whole frequency range, so we get that the auto regressive prediction value consists completely of a linear combination of observational data. The gain is from 0.8 to 0.9, and the angle of lag of the phase is about 0.4 radian in the band-width where the power spectrum is reduced to 6db. Taking into account these characteristics in the frequency domain, we can get that the auto regressive prediction for random error series of night time position line at Rishiri in the band-width is done completely. On the other hand, the gain and the phase fall into confusion in high-frequency range. But it is out of the question for the reason that percentage of power component in high-frequency range is below 1%.

We fixed a ship's position by the intersecting point of two position lines, so it is necessary for us to investigate the parameter of controlled error ellipse in order to examine the improvement of a ship's position. The conjugate semidiameter a_x^*, a_y^* of controlled error ellipse is reduced to 42%, 27% and the area S^* is reduced to 11% compared with the uncontrolled error ellipse.

(2) *The results of Red and Green lanes at Okushiri by using the auto regressive model at Hakodate which is the monitoring point*

The auto regressive model of Red and Green lanes at Hakodate is given by

$$Z_r(s) = 0.94481Z_r(s-1)+U_r(s)$$

$$Z_g(s) = 1.00046Z_g(s-1)+0.13063Z_g(s-2)+0.16634Z_g(s-3)$$
$$-0.15262Z_g(s-4)+0.06020Z_g(s-5)+U_g(s)$$

Fig. 4–7 and Fig. 4–8 show the observational random error series, the auto regressive prediction series and the prediction error series of Red and Green lane at Okushiri, July 28–29, 1976. The standard deviation of prediction error of Red lane becomes 0.19 lane and the one of Purple lane is 0.13 lane, though the standard deviation of observational random error series of Red lane is 0.39 lane and the one of Purple lane is 0.31 lane. This fact shows that the estimstion function ε_r, ε_g is equal to 0.49, 0.58 and the variation of random error series of night time position line at Okushiri reduced to one-half.

Fig. 4–9 and Fig. 4–10 show the power spectrum and frequency response function at Okushiri. The power spectrum of observational data has the greater part of energy in low-frequency range the same as that of the power spectrum at Rishiri. The power spectrum of prediction error has a tendency to increase in high-frequency range preferably. So it is evident that the variation of random error series on low-frequency range where the power spectrum has the greater part of energy is eliminated completely. The coherency is 0.96 in the whole frequency range, so we get that the auto regressive prediction value consists completely of a linear combination of observational data. The gain is 0.9 and the angle of lag of the phase is from 0.4 to 0.6 radian in the bandwidth. Taking into account these characteristics in

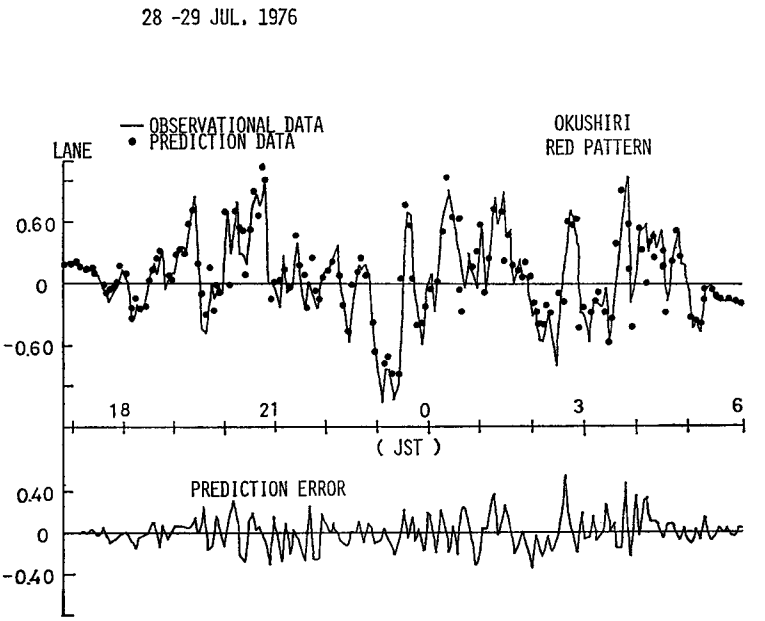

Fig. 4–7. Time history of observational position line, prediction data and prediction error. (1630–0600)

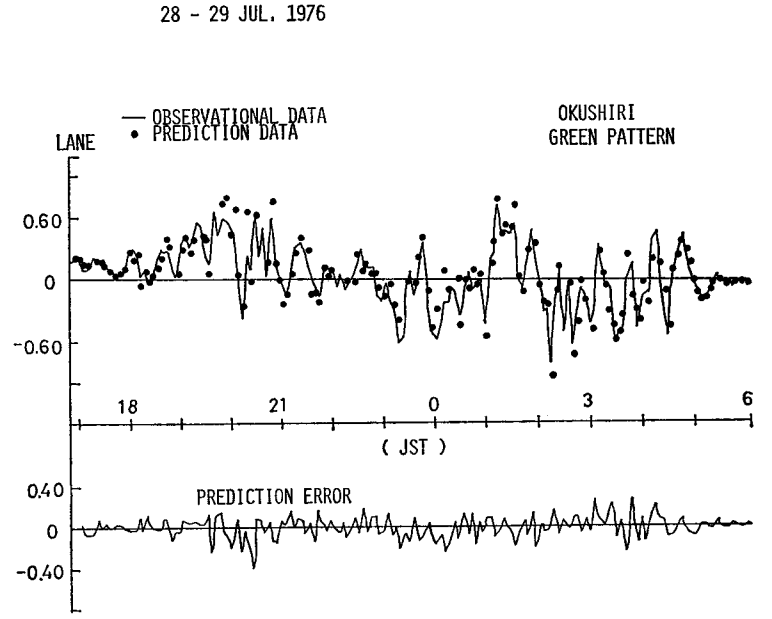

Fig. 4–8. Time history of observational position line, prediction data and prediction error. (1630–0600)

the frequency domain, we get that the auto regressive prediction for random error series of night time position line in the band-width is well done as well as at Rishiri. On the other hand, as stated before, the power spectrum of prediction error has the tendency to increase in high-frequency range. We have the interpretation about it according to the frequencu response characteristics that the variation of random

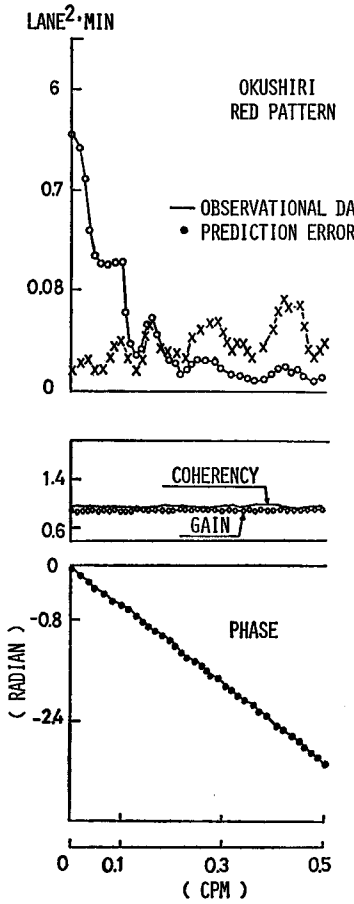

Fig. 4–9. Power spectra, response characteristics and coherency between observational data and prediction data.

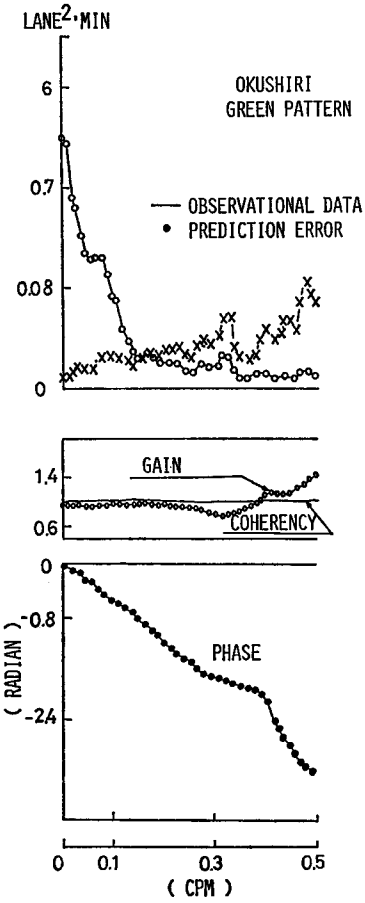

Fig. 4–10. Power spectra, response characteristics and coherency between obse rvational data and prediction data.

error series at Okushiri has the greater energy comparatively from 0.03 CPM to 0.1 CPM and the auto regressive prediction can't follow the variation in such frequency range, so the power spectrum of prediction error has a tendency to increase the short-period power component. Other observational points such as Akkeshi and Shakotan have similar results, so we can conclude that the optimal

linear controlled value by means of auto regressive prediction has its limit to the random error series which has the greater energy comparatively in the IF range. But it cuts a small figure in our study for the reason that percentage of power component in IF and high-frequency range is from 1% to 10%.

The conjugate semideameter (a_x*, a_y*) of controlled error ellipse is reduced to 51%, 42% and the area S* is reduced to 28% compared with the uncontrolled error ellipse.

(3) *The results of Red and Purple lanes at Moura by using the auto regressive model at Hakodate which is the monitoring point*

The auto regressive model of Red and Purple lanes at Hakodate is given by

$$Z_r(s) = 0.99447Z_r(s-1)-0.17133Z_r(s-2)+U_r(s)$$

$$Z_p(s) = 0.87552Z_p(s-1)-0.05102Z_p(s-2)+0.05132Z_p(s-3)$$

$$\vdots \qquad \vdots \qquad \vdots$$

$$-0.03564Z_p(s-36)+0.19135Z_p(s-37)+U_p(s)$$

Fig. 4–11 and Fig. 4–12 show the obervational random error series, the auto regressive prediction series and the prediction error series of Red and Purple lane at Moura, August 12–13, 1976. The standard deviation of prediction error of Red lane becomes 0.09 lane and the one of Purple lane becomes 0.10 lane, though the

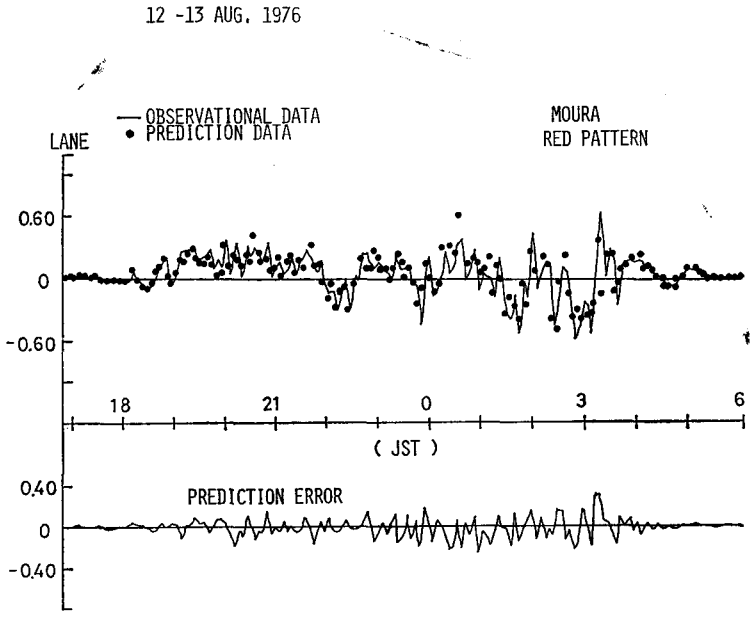

Fig. 4–11. Time history of observational position line, prediction data and prediction error. (1630–0600)

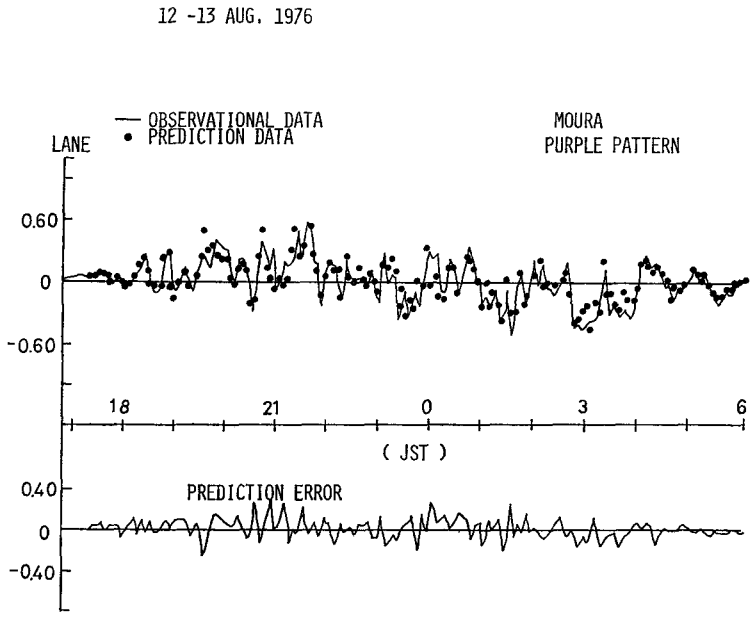

Fig. 4–12. Time history of observational position line, prediction data and prediction error. (1630–0600)

standard deviation of observational random error series of Red lane is 0.17 lane and the one of Purple lane is 0.20 lane. This fact shows that the estimation function ε_r, ε_p is equal to 0.53, 0.45 and the variation of random error series of night time position line at Moura is reduced to one-half.

Fig. 4–13 and Fig. 4–14 show the power spectrum and frequency response function at Moura. The observational data have the greater part of energy in low-frequency range, especially from ultra-low-frequency range to 0.1 CPM. The power spectrum of prediction error equally has small energy through the whole frequency range. So it is evident that the variation of random error series in low-frequency range where the power spectrum has the greater part of energy is eliminated completely as well as at Rishiri and at Okushiri. The coherency of Red lane is 0.98 in the whole frequency range, so we get that the auto regressive prediction value consists completely of a linear combination of observational data. The gain is 0.95 and the angle of lag of the phase is 0.6 radian in the band-width. Taking into account these characteristics in the frequency domain, we get that the auto regressive prediction for random error series of night time position line at Moura in the band-width is well done.

The coherency of Purple lane is 0.9, the gain is 0.95 and the angle of lag of the phase is 0.6 radian, so we get that the auto regressive prediction for random error series of night time position line of Purple lane in the band-width is well done. On the other hand, the gain, the coherency and the phase are distributed in high-

frequency range. It is natural to consider that these disturbances are due to the large order (37) of auto regressive model of Purple lane. As mentioned before, The little aptitude of auto regressive model in high-frequency range is out of the question. But when we regard our study as the adaptive control of random error

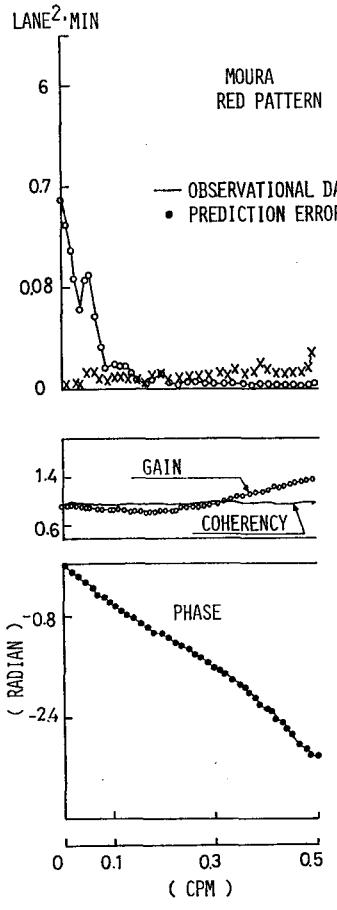

Fig. 4–13. Power spectra, response characteristics and coherency between observational data and prediction data.

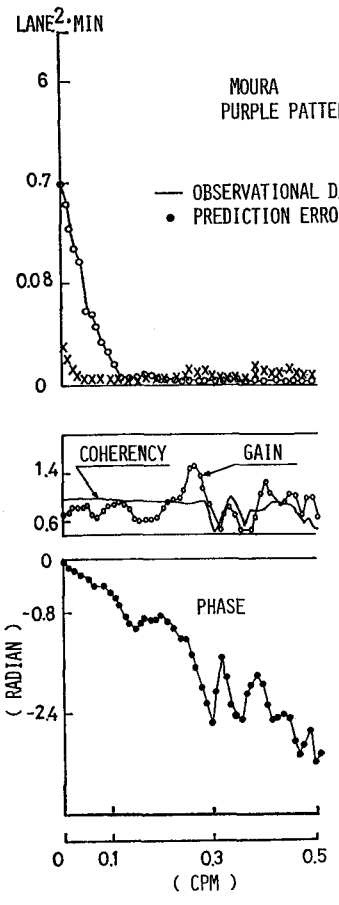

Fig. 4–14. Power spectra, response characteristics and coherency between observational data and prediction data.

series in high-frequency range where the power spectrum has nothing but small energy, we had better adopt the auto regressive moving average model which can cover a wider random process. It is the subject for further research. The conjugate semideameter (a_x*, a_y*) of controlled error ellipse is reduced to 47%, 55% and the area S* is reduced to 24% compared with the uncontrolled error ellipse.

4-8 Time-Space coverage of auto regressive model at monitoring points

(1) *Space coverage of auto regressive model*

In section 4–7, we discusses the result of the adaptive control for random error series of night time position line at a fixed point by monitoring method, and it has been definitely shown by the estimation function that the variation of random error series is reduced from one-half to one-third. In this section, we discuss the space coverage of auto regressive model on the occasion of setting the monitoring point in order to control the random error series in the whole sea area of Hokkaido.

Table 4–1 shows the three-way layout of estimation function where the factor A is the monitoring point, the factor B is the lane of position line and factor C is the observational point for control. Table 4–2 shows the analysis of a variance table of the parametric model and we get the following knowledges:

(a) We can't recognize any significance among factor A. That is to say, whichever monitoring point we take (Hakodate, Kushiro, Wakkanai), there is no significance among the estimation function.

(b) We can evidently recognzie some signfiicance among factor B. That is to say, there is a significance among the estimation function of each line. This is due to the fact that the larger random error series vary, the more effective the adaptive control works on. It is evident by Fig. 4–15 that the estimation function is inversely proportional to the standard deviation of random error.

Table 4–1. *A list of three-way layout.*

Lane	O. point	S.d.	Hakodate	Kushiro	Wakkanai
Red	Hakodate	0.28 lane	0.31	0.32	0.33
	Kushiro	0.13 lane	0.53	0.54	0.52
	Wakkanai	0.14 lane	0.42	0.43	0.43
Green	Hakodate	0.11 lane	0.32	0.34	0.31
	Kushiro	0.09 lane	0.42	0.43	0.39
	Wakkanai	0.03 lane	0.51	0.48	0.48
Purple	Hakodate	0.20 lane	0.39	0.41	0.40
	Kushiro	0.42 lane	0.27	0.26	0.25
	Wakkanai	0.27 lane	0.27	0.26	0.26

Table 4–2. *Analysis of variance table.*

Factor		ϕ	V	F_0	5%	1%
(A)	0.00	2	0.0000	0.00	4.74	9.55
(B)	0.06	2	0.0300	21.43**	4.74	9.55
(C)	0.00	2	0.0000	0.00	4.74	9.55
$(A\times B)$	0.00	4	0.0000	0.00	4.74	9.55
$(A\times C)$	0.01	4	0.0025	1.79	4.12	7.85
$(B\times C)$	0.16	4	0.0400	28.59**	4.12	7.85
(e)	0.01	7				
Total	0.24	27				

(c) We can't recognize any significance among factor C.
(d) We can't recognize any significance in A and B interaction (the monitoring point X each lane) and in A and C interaction (the monitoring point X the observational point for control), but we can recognize some significance in B and C interaction (each lane X the observational point for control). This is caused by the reason of (b). according to the above results, it is evident that whichever monitoring point we take, there is no significance among the estimation functions, so we can control random error series in the whole sea area of Hokkaido by using only one monitoring point.

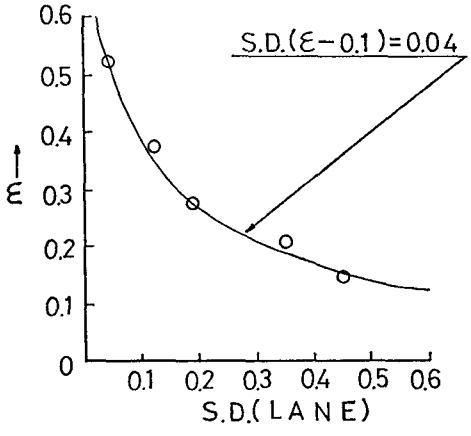

Fig. 4–15. Relationship between ε and standard deviation

(2) *Time coverage of auto regressive model*

The time coverage of auto regressive model depends on the time-varying order of auto regressive model. Fig. 4–16 shows the change of order in a

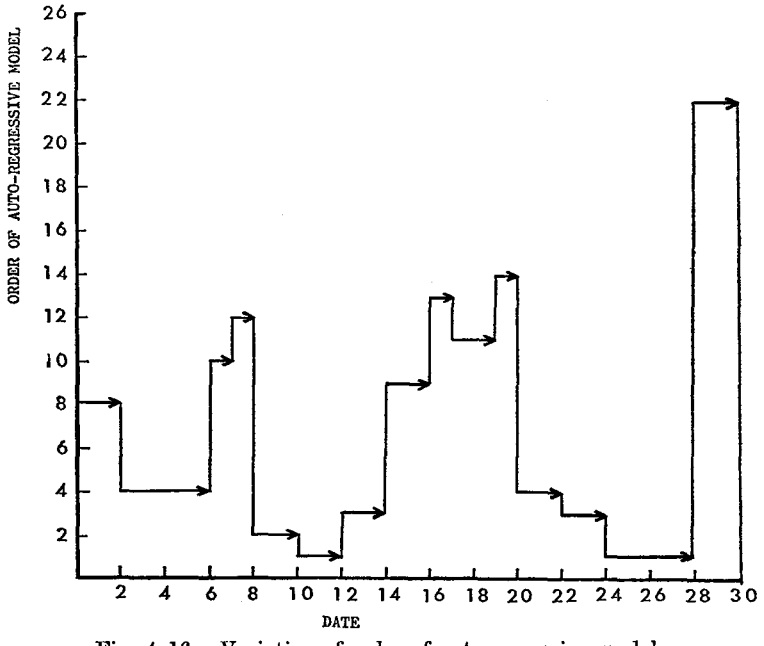

Fig. 4–16. Variation of order of auto regressive model.

month at Hakodate, March, 1976. The time coverage of auto regressive model for random error series of night time position line is from two days to four days, and some of them change every day.

In order to control the random error series, we first set the auto regressive model at the monitoring point, and next we decide the optimal linear controlled value by means of its auto regressive model. So it is necessary to get time lag between modeling and control. The time coverage of auto regressive model at the monitoring point is concerned with the time coverage of auto regressive model which we appropriate to the control of random error series, and it is to be desired that time coverage of auto regressive model at the mointoring point be long. But by Fig. 4–16 the time coverage of auto regressive model of a previous day at the monitoring point is suited to control random error series of night time position line.

5. Conclusion

We first analyze the random error series of night time position line by means of time series analysis, and then we try to control the random error series at a fixed point by the monitoring method.

1 The results of time series analysis for random error series of night time position line

The random error series of night time position line for the Decca system consists of many low-frequency components and a few high-frequency components. The power component of Green lane is the smallest of the three through the whole frequency range, and it seems that this is caused by the location of a transmitting station, the propagation characteristics of $9f_0$ and the multiple number of $9f_0$.

The power component of random error series of night time position line shows the seasonal variation which has a tendency, summer>autumn, spring>winter, especially in low-frequency range.

The standard deviation of random error series of night time position line must be kept less than 0.45 lane in order to hold the slip-lane.

2 The results of time series analysis between field strength and position line

The field strength of a Decca signal which is transmitting far from the Decca station at night is Lailei distributed. On the other hand, the field strength of a Decca signal which is transmitting near the station is Gaussian distributed.

The normalized time series of field strength indicates that almost-periodic data have the greater part of energy in low-frequency range, as well as random error series of night time position line.

The linear relationship between the time series of field strength and the one of position line in low-frequency range where the power spectrum has the greater part of energy is very low.

3 Adaptive control for random error series of position line which is observed at a fixed point by the monitoring method

We get tht random error series of night time position line at three observational points (Rishiri, Okushiri and Moura) being reduced from one-half to one-third. Also according to the frequency response function between the observational random error series and the auto regressive prediction series, it is evident that the adaptive control for random error series is completely done in the band-width where the power spectrum is reduced to 6db.

On the other hand, when the variation of random error series has large energy from 0.03 CPM to 0.1 CPM and when it has a large order of the auto regressive model, the effect of control has a tendency to decrease in high-frequency range. But it is out of the question for the reason that percentage of power component in high-frequency range is from 1% to 10%.

Whichever monitoring point we take, there is no significance among the estimation function, so we can control the random error series in the whole sea area of Hokkaido by using only one monitoring point.

The time coverage of auto regressive model is short and some of them change every day, so the auto regressive model of a previous day at the monitoring point is suited to control.

At the traditional Navigation the study of random error of position line is treated as statistical characteristics of Descriptive Statistics. But in this study we treat the random error series as a stockastic process, and analyze the characteristics of the same in the frequency domain by means of time series analysis.

Furthermore, we formularize the decreasing of random error series as the adaptive control, and can get good results. We can't refer to the auto regressive moving average model on the occasion of an increasing order of auto regressive model in this study, so it is the subject for further discussion.

References

1) Yamakoshi, Y. (1976). The test of the Hokkaido Decca chain. *SANE* **67-14**.
2) Hirota, T. (1969). The test of the Hokkaido Decca chain. *SANE* **68-24**.
3) Yutaka, K. (1968). The result of measurement of the Hokkaido Decca chain. *Radio Navigation*. **9**, 4–8.
4) Yutaka, K. (1969). The test of measurement of the Hokkaido Decca chain No. 2. *Radio Navigation*. **10**, 4–10.
5) Watanabe, Y. (1965). The relationship between the R.M.S. field strength of sky wave and the phase. *The Decca technical data* **203**, Navigation Aids Department of The Maritime Safety Agency.
6) Navigation Aids Department of The Maritime Safety Agency. The Decca correction chart–1138.
7) Kawaguchi, S. and Ishida, M. (1974). On the statistical properties of decometer readings for Decca system in the night –I. *J. Naut. Sco. Japan*. **52**, 95–100.
8) Kawagichi, S. and Ishida, M. (1977). On the statistical properties of decometer readings for Decca system in the night –II. *J. Naut. Soc. Japan*. **57**, 33–46.
9) The Radio Research Laboratories. Ministry of Posts and Telecommunication. Ionospheric Data in Japan.

10) Nara G. (1966). Studies on the measurement and display on irregular surfices. *Report of the N.R.L.M.* Oct. 19–27.
11) Cartright, D.E. and Longuett-Higgins, M.S. (1956). The statistical distribution of maxima of random function. *Proc. Royal. Soc.*, **237**, 212–232.
12) Amagai, K. (1972). Study on the dynamic response between a ship's motion and fishing gear (II). *Bull. Fac. Fish. Hokkaido Univ.* **23**. 102–126.
13) Rice, S.O. (1945). Mathematical analysis of random noise *Bell Syst. Tech. Jour.*, **23**, 282–332.
14) Rice, S.O. (1948). Statistical properties of sine-wave plus random noise. *Bell. Syst. Tech. Jour.*, **27**, 109–157.
15) Middleton, D. (1946). The response of biased saturated linear, and quadratic rectifieres to random noise. *Jour. Applied Physics.* **17**, 778–801.
16) Middleton, D. (1948). Some general results in the theory of noise thorough nonlinear devices. *Quart. Applied Math.*, **5** 445–498.
17) Norton, K.A. (1952). Probability distribution of the phase of the resultant vector sum of a constant vector plus a Raylei distributed vector. *J. Applied Physics.* **23**, 137–141.
18) Norton, K.a. (1955). The probability distribution of the amplitude of a constant vector plus a Rayleigh distrubuted vector. *IEE.* Oct. 1354–1361.
19) Hannan, E.J. (1970). *Multiple time series.* John Willy & Sons. Now York.
20) Enochson, L.D. (1969). Frequency response functions and coherency functions for multiple input linear ststem. *NASA* **CR-32**. 21–47.
21) J.S. Bendat and A.G. Porsol. (1971). *Random data.* John Willy & Sons. 156–169.
2) Kawaguchi, S. and Ishida, M. (1977). Adaptive control for random errors of Decca system, which is observed at the fixed point in the night. *J. Naut. Soc. Japan.* **57**, 17–31.
23) Box, G.E.P. and Jenkins, G.M. (1962). Some statistical aspects of adaptive optimization and control. *J.R. Stat. Soc.* **24**, 297–343.
24) Box, G.E.P. and Jenkins, G.M. (1963). Further contribution to adaptive control: Simultaneous estimation of dynamics, non zero costs. *Bull. Inst.* **40**, 943–947.
25) Akaike, H. (1970). Statistical prediction identification. *Ann. Inst. Statist. Meth.* **22**, 203–217.
26) Akaike, H. (1972). *Statistical analysis and control of dynamic system.* Science Inc. Tokyo.
27) Tokumaru, H (1976) The model of the environmental pollution and the environmental design: prediction model and design. *Automatic control technique.* **22**, 69 –78.